ANNUAL REPORT FOR YEAR 2

for

# APPLICATION OF REMOTE SENSING TO STUDY NEARSHORE CIRCULATION

under Grant NASA-NGL 47-022-005

John Zeigler, Principal Investigator

with

Larry Haas
Robert Lobecker
Donald Stauble
Christopher Welch
C. S. Fang

Virginia Institute of Marine Science
Gloucester Point, Virginia 23062

September 1974

TABLE OF CONTENTS

LIST OF TABLES

LIST OF FIGURES

LIST OF FIGURES (Cont'd)

## SUMMARY

Within the second year of research it became plain that user application of remote sensing techniques being developed in this contract on the continental shelf, both physical and biological, were still a few years away even with the frenzy of OCS activity associated with search for oil. It also became plain that the single most important physical process required by users in the marine environment is circulation and dispersion information. Circulation is difficult to study at best and remote sensing appears to be the most promising tool. Unfortunately circulation studies, where cost must be kept modest, require development of new techniques and the time required to do this poses a serious problem for contractural work which expects yearly user application of the techniques.

User requirements in the lower Chesapeake Bay, however, in contrast to the continental shelf are manifold and increasing. Requests for assistance from cities, state agencies, and others are arriving weekly. Last year (the first year of this contract), for example, we were able to respond to the Navy, the Virginia Department of Highways and the Hampton Roads Sewer District, using the remote sensing techniques being developed for the continental shelf by this contract.

Given this present real world situation, in which the greatest need for user application of remote sensing lies not on our adjacent continental shelf but within the estuary, a decision was made to shift the emphasis of this contract away

from the continental shelf into the lower Chesapeake estuary where user needs are great and where, therefore, the remote sensing techniques would have the best chance for immediate application. In this sense we hope to maximize both the user application and our chances to fulfill the requirements of the granting agency.

Work done developing drogues and the Omega navigation system will not be lost because both are highly useful within the estuary. Furthermore, the increase in activity on the continental shelf implies that user needs will dramatically increase there in the next few years.

This decision appears to have been wise because since June (the beginning of the current year) we have had two occasions to respond to user needs and one of these will result in placement of engineering works, but this is a story for next year's report.

The following work was pursued in the past year:

1.) Continued development of the Omega system.

2.) Coordinated study of Wachapreague Inlet:

Biological
Hydrological
Sedimentation

3.) Continental shelf current studies:

1.) Field support for SKYLAB mission

2.) Continuous deployment of EOLE buoys with NASA/Langley.

The above topics are presented in complete detail as an appendix to this report.

Omega System

From the inception of this grant it has seemed to us that understanding of most water quality problems is limited by lack of understanding of circulation. We still believe this to be true. From the beginning we have sought to use a remotely sensed drogue which would have the following qualities:

1) Cheap; 2) versatile in that it could respond to satellites, or aircraft, or boats; 3) be useful as a platform for collecting more than one kind of data.

After considerable thought we settled on the Omega System for Navigation. Unfortunately, the manufacturer had oversold his product. He was a full year late in delivery and the units were not in working order upon arrival. In any event, the past year was one of frustration; however, the system is now in one place and the transmitter under contract to be delivered in September 1974.

Given this situation, field trials are planned for autumn 1974, and if all goes well the Omega System should be a functional tool by winter. With this in mind, we anticipate writing a contract proposal to support the system and use it to the appropriate interested agency, such as ONR or MARAD.

Wachapreague Inlet

When the second year began our thinking was still on nearshore circulation on the continental shelf. Within the limits initially defined in this contract it was plain that nearshore circulation would be strongly influenced by inlets.

The whole Eastern Shore is perforated by inlets. Therefore, it was decided to study a single inlet, the best known one, and determine the biological, hydrographical and sedimentological interactions. A three year study of Wachapreague Inlet had just ended, considerable logistical support in boats and people were available, so we elected Wachapreague as the prototype.

The biological studies were designed with the following objectives in mind:

a.) Is there a net flux of organic material from the inlet to the ocean?

b.) What biological parameters can be used to distinguish between nearshore waters and marsh waters?

c.) What is the best parameter for remote sensing to answer the above?

Measurement of net flux was not possible, given the time and effort prior to the decision to abandon the shelf. Flux is extremely difficult to measure even when the substance is pure water. Progress however was sufficient that a new proposal is being written solely to study flux.

Chlorophyl per se proved not to be a reliable indicator to distinguish between seawater and marsh water because of general high turbidity. Variations in heterotrophic metabolism, however, was useful. This conclusion left the answer to a remote sensing parameter unanswered; however, with the decision to work this third year within the estuary, the usefulness of chlorophyl will probably be enhanced because of

its relationship to plankton blooms and a possible relationship between blooms and pollution.

Sediment Plume

Marsh water is more turbid than ocean water and therefore a plume of discolored water is discharged from the inlet on ebb tide. The plume is visible and therefore can be examined by several remote sensing techniques. In the case of Wachapreague we used a series of photographs from three missions flown by NASA/Johnson Spacecraft Center and thermal imagery which when enhanced by NASA/Houston was suitable for measuring temperature contrasts between the plume and seawater.

The shape and behavior of the plume proved to be the best index of interaction between inlet and nearshore circulation. Although the program did not continue long enough to discover why volume of sediment calculated from remote imagery did not fit previous theory. Thermal imagery followed very well the visible plume and we conclude that it would be a prime tool for nearshore circulation studies. The results showed that indeed there was strong thermal contrast between seawater and marsh water.

Continental Shelf Current Studies

When the second year began this was the principal objective. Lacking the Omega Navigation System the researchers had to do other experiments. The first was a SKYLAB mission which required ground truth near the mouth of the Chesapeake Bay. The field team assembled and used the Radar Drogue System

developed the year before with assistance from NASA/Langley and NASA/Wallops. The results were given to Dr. Maynard Nichols of VIMS, who was the SKYLAB principal investigator for this mission.

A greater effort went into the EOLE drifting buoy program as a joint effort between NASA/Langley and VIMS. These buoys are tracked by the NASA funded French Satellite and the results thus far are to provide the most concrete picture of currents on the continental shelf off Virginia. Currents tend to move southerly to Cape Hatteras and become entrained in the Gulf Stream at that point from whence they turn northeast and move rapidly out of our area. These background studies will prove extremely valuable for future programs on the continental shelf and would have been basic in experimental design.

A critical response to user request arose from these studies although it would be stretching a point to claim Application of Remote Sensing Techniques for the response. The Hampton Roads Sewer District proposes to construct an ocean outfall at Dam Neck. This area is right in the center of the EOLE program. Dr. Welch analyzed existing data and pointed out that the proposed outfall could result in the beaching of effluent. As a result HRSD has contracted further studies with Alpine Geophysical and Hydrosciences, Inc., to determine what might best be done. A copy of Dr. Welch's report was sent to you in this year to keep you informed.

All in all then, these lessons are to be transferred into the lower Chesapeake Bay for application. Already they have been applied and the advice derived from them translated into dollars and cents engineering.

APPENDIX 1

## THE STUDY OF NEARSHORE CIRCULATION IN THE VICINITY OF A NATURAL TIDAL INLET BY REMOTE SENSING TECHNIQUES

### Object

The object of this study was to investigate the use of remote sensing in the study of nearshore circulation in the vicinity of a natural tidal inlet. An economical technique was needed to investigate changes in the entire visible and temperature plume, characteristic of nearly all tidal inlets, thru at least one tidal cycle. The importance of this endeavor is to study the extent of influence the visible and temperature plume has on nearshore circulation thru changes in plume structure and indirectly in transport of sediment in and out of inlets. Due to the large area of plume influence even in moderate size inlets it was hoped that remote sensing techniques would be the most desirable method to cover the entire area of study for the required length of time.

The study area was located at Wachapreague Inlet, a natural tidal inlet with little man-made influences, on the Eastern Shore of Virginia. This inlet was the site for several previous studies on inlet dynamics by institute personnel.

### Results

A complete tidal cycle of twelve hours was photographed by aircraft supplied by NASA/Johnson Spacecraft Center on 6 April, 7 August, and 17 November 1973. Color film, color infrared film and thermal scanner imagery were supplied on these missions.

The color infrared film supplied the best imagery of the visible turbidity plume.

The growth sequence of a large, well developed turbidity plume was photographed during the ebb tidal cycle on 6 April. The decay sequence of a smaller, less developed turbidity plume was photographed during the flood tidal cycle on 7 August. Weather limitations negated the use of the third series of photographs. Calculations of the changes in area in the turbidity plume were determined for the usable portions of the tidal cycle from the color infrared film. The volume of the water column from surface to bottom contained within the plume boundary was computed and compared with the estimated volume storage of the Wachapreague Inlet storage system in the marsh landward of the inlet which was developed previously by Dr. R. Byrne and M. Penney of the Institute. It can be inferred by the poor correlation between the computed volume and the storage system volume that while the suspended sediment is relatively homogeneously mixed throughout the water column in the throat of the inlet, as the turbidity plume expands seaward over the ebb tidal delta, there is mixing of sediment laden inlet water with ocean water. The results show that the imagery allows estimation of turbidity depth once a storage volume graph has been developed for a particular inlet system.

The thermal imagery was inhanced and rectified in order to investigate the relacionship of the visible turbidity plume with the sensed thermal plume. Water directly related with the inlet-marsh storage system will have a different temperature

from the surrounding ocean water and be delineated by a thermally sensed plume. Comparison of the area of the thermally sensed plume with the area of the visible turbidity plume shows a good correlation. However, the surface structure of the thermal plume is more complex than the visual turbidity plume. This thermal image structure was then analyzed by visual methods directly from the inhanced and rectified film and also by density slicing technique. While visually analyzing the thermal imagery for the ebb tidal cycle several concentric bands developed with alternating moderate to cool water which expanded as the tide ebbed.

Using the color encoding densitometer on the thermal imagery gave the most complete picture of a complex thermal structure. More detail could be distinguished on the concentric bands with the warmest relative temperature in the inlet and progressively cooler bands radiating seaward from the inlet mouth. A tongue of cool oceanic water can be seen progressing up-coast, bisecting the thermal plume during the ebb tidal cycle. A distinct body of warm water, possibly from a preceding tidal cycle, was visible proceeding seaward and slowly cooling as the tidal cycle progressed.

Future

This research shows that remote sensing is a viable tool in the study of nearshore circulation in the vicinity of tidal inlets. The work will continue at a low level for lack of immediate technology transfer. Information gained through this

research will, however be of value in future remote sensing projects.

## Introduction

Nearshore circulation in the vicinity of a natural tidal inlet has been studied by remote sensing. From three separate series of sequential aerial photographs, it was possible to document a complete tidal cycle and evaluate the nearshore influences of such circulations. Using aerial photographs, it was possible to compute the relative changes in the area and total volume of the suspended sediment plume during the tidal cycle and compare them to a known approximate storage volume function of the complex inlet-marsh storage system. Comparison of the visual turbidity plume from color photography with the thermal plume from thermal imagery was also accomplished.

The study area was located at Wachapreague Inlet in the barrier island chain on the Eastern Shore of Virginia. This inlet is a good example of a downdrift offset inlet common along this coast (Fig. 1.1). The inlet is bordered on the north by Cedar Island and on the south by Parramore Island. The morphology of this inlet consists of an inlet throat channel, a well-developed crescentic ebb tidal delta on the east and a system of bays, marsh and tidal channels to the west. The inlet throat channel reaches a maximum depth of some 65 feet, while the ebb tidal delta has a depth on the order of twelve feet (Fig. 1.2). Rapidly changing shoals periodically above sea level are present on the north side of the inlet

throat channel with smaller shoals on the south side just off Parramore Island. The nearshore shelf bathymetry is relatively smooth landward of the 36 foot contour. Complex ridge and swale topography with a rough northeast lineation is found seaward of the 36 foot contour. The interested reader is referred to a study by DeAlteris and Byrne (1973) and Byrne, Bullock and Tyler (1973) on the recent history and response characteristics of Wachapreague Inlet.

Experimental Procedure

Three photographic missions were flown by NASA/Johnson Spacecraft Center on 6 April, 7 August and 17 November, 1973. A complete tidal cycle of twelve hours was covered on these three days. Each phase of the tidal cycle photography consisted of three overlapping flyovers of the southern, middle and northern portions of the inlet and marsh system. The center flight path photographs were used whenever possible in this study. The aircraft was equipped with color film, color infrared film and thermal scanner. The photo scale was 1:40,000 on the 6 April, 7 August and the first run of 17 November. The remaining photographs of 17 November are at a scale of 1:30,000. On 6 April, four passes of the ebb tidal cycle were photographed at 1106, 1225, and 1346 and 1504 EST. The flight lines are shown in Figure 1.3. The 7 August series consisted of one late phase of the ebb tidal cycle photographed at 0720, low tide photographed at 0820, and three series of photographs of the first half of flood tide at 0910, 1000, and 1058 EST. The flight lines are shown on Figure 1.4. The

17 November series consisted of three passes of the flood tidal cycle which were photographed at 1033, 1124, and 1240, high tide photographed at 1342, and one phase of ebb tide at 1435 EST. The flight lines are shown in Figure 1.5.

Description of Raw Data

A large, well developed plume of suspended sediment originating in the marsh was readily visible flowing out of the inlet mouth and expanding during the ebb tidal cycle on 6 April. A smaller suspended sediment plume was observed to decrease in area during low slack water and first half of the flood tidal cycle on the 7 August photographs. The outline of the visible sediment plume was traced on clear acetate overlay paper from the aerial photograph for each hour of the tidal cycle flown. Unfortunately, a turbidity plume was not visible on the 17 November flood tidal cycle photographs due to morning cloud cover and high northwest winds, possibly dissipating the surface structure of the plume. Therefore, calculations of changes in the turbidity plume during this portion of the tidal cycle could not be determined.

A detailed bathymetric map of Wachapreague Inlet (Fig. 1.2) was constructed at three foot depth intervals using U. S. Coast and Geodetic Survey hydrographic sounding sheets numbers 5674, 5703, 5715 and 5770 (scales of 1:40,000 and 1:20,000) done in 1934. Detailed bathymetry at the Inlet proper was constructed originally at a scale of 1:10,000 from field data collected by VIMS personnel on 11 and 12 December 1972. A boat equipped

a Fathometer and Radar Transponder was located in the inlet by radar equipment located at the town of Wachapreague supplied by NASA/Wallops (see Welch and Haas, 1973).

Analysis Technique

A Map-O-Graph was used to bring the various scales of the charts and overlays into one common scale of 1:16,400. The outline of the suspended sediment plume for each portion of the tidal cycle could then be plotted over the bathymetry.

These constructed plots of the outline of the sediment plume over the bathymetry for each hour of the tidal cycle were planimetered at three foot contour intervals to compute the area of the plume seaward from the inlet mouth. When multiplied by the three foot depth interval, the volume of the water column from bottom to surface was computed. This volume was originally hypothesized to contain the complete suspended sediment plume for each phase of the tidal cycle.

This volume was then compared with the estimated volume storage of the Wachapreague Inlet storage system, computed from a graph developed by Byrne and Penney (1974) relative to the tide gage at the town of Wachapreague. The tidal height at the time of each aerial photograph was read off a strip chart from a tide gage located at the inlet. In order to use the graph, the time of readings on the Wachapreague Inlet tide gage had to be corrected for a phase lag, between high and low waters of -0.6 hrs and -0.7 hrs, respectively, to the town of Wachapreague tide gage, approximately 12 km distant via channels from the inlet. A height correction was also needed due to an 0.5 ft

difference in height to mean low water between the two tide gages.

Results

The progressive increase in area of the well developed suspended sediment plume on 6 April is seen in Figure 1.6 as the ebb tidal cycle progressed. The wind on that day was out of the northwest between nine to fifteen MPH at the time of the photography, which may have some relation to the plume formation. Storm conditions prevailed for several days prior to the photographs, causing the entire marsh area between Wachapreague and Parramore Island to be flooded at high tide, which allowed a large amount of sediment to be placed in suspension in the system. From Figure 1.6 and Figure 1.7 it is noted that the seaward edge of the plume developed a finger-like structure from 1346 on. It was noted above that the ridge and swale bathymetry develops seaward of the thirty-six foot contour (Fig. 1.2). The orientation of the fingers of suspended sediment are roughly parallel to these northeast trending ridges.

Contrasting the large change in plume area during the ebb on 6 April, the changes of the suspended sediment plume on 7 August 1973, during the last stage of ebb, low, and first half of flood tides are illustrated in Figure 1.8 as being extremely small until 1058, approximately 3 hours after low tide. The 7 August plume at its maximum area was approximately four times less than the maximum area of the 6 April plume.

Figure 1.9 shows the shape of the suspended sediment plume during the flood cycle on 7 August, as contrasted to the shape of the ebb plume of 6 April (Fig. 1.7). It can be noted from Figure 1.8 that there was relatively little change in the total area of the plume on 7 August during that series of photographs, although it covered the tidal cycle from ebb through low to flood. The wind on that day was calm to 5 MPH from the southeast. The area of the plume increased toward low tide to its maximum at 0820 EST, then decreased for one hour of flood as expected but anomalously increased almost to its maximum low tide area again at 1000 EST; then decreasing rather rapidly within the next hour of flood. The maximum area of change during this time was observed at the inlet flanks of the plume, of special note being the northern flank between the shoal and Cedar Island Beach. The "V" shaped plume edge can be seen migrating slightly seaward to low tide and then reversing to migrate into the beach approximately 1 nautical mile north of the inlet at 1058. The main flow at 1058 is through the throat of the inlet.

Interpretation

There was generally poor correlation between the volume of the suspended sediment plume calculated by the above described method and the volume calculated in the storage system by the method of Byrne and Penney (1974). The suspended sediment concentration in the plume was assumed to be constant with the total volume of the plume from surface to bottom. From Table 1.1

it can be seen that the volume of the plume was close to the volume of the storage system for the first hour of ebb studied on 6 April and again on the last hour of flood on 7 August. At both of these times the suspended sediment plume was basically confined to the main inlet throat channel and the landward edge of the ebb tidal delta. It can be assumed that in this region the suspended sediment concentration is relatively homogeneous throughout the water column. As the suspended sediment plume expands seaward over the ebb tidal delta, there is mixing of the sediment laden water of the inlet with ocean water. A hypothetical cross-sectional structure is illustrated in Figure 1.10 with a homogeneous concentration landward of the ebb tidal delta, with a distinctly less homogeneous plume of turbid water over clear ocean water seaward of the delta.

To compute a relative depth of suspended sediment, the change in the calculated volume of the storage system between successive photographs was divided by the change in the measured area of the plume between successive photographs. From Table 1.1 the average depth of the plume appears to be 22 ft on 6 April and 29 ft on 7 August. The anomalously low number of 6.18 ft between 1346 and 1504 on 6 April 1973 accompanies an increase in area of the plume by a factor of 2. The anomalous depth of 18.92 ft at 0820 on 7 August occurs at low tide when the system is changing from one of ebb to one of flood. Another anomalous depth occurs when the area of the plume first decreases then increases on the beginning stage of

flood tide. From the photos at 0910 and 1000, the plume appears to increase in area at both the northern and southern flank of the inlet. Thus, the large number of 88.81 comes from the fact that both the area of the plume and storage volume are increasing at the same time which is opposite the standard condition where on a flooding tide the plume area should decrease with time.

The depths computed here are only "relative" depths since no profiles of suspended sediment concentration were collected at the time of the overflights. The results show that the imagery allows estimation of turbidity depth once the storage volume for the special area has been computed.

Thermal Imagery

Thermal imagery was recorded concurrently with the photography for all of the overflights. The thermal imagery for the 6 April 1973 flight was enhanced by NASA/Houston to gain the maximum contrast between plume water and ocean water. The central 40° of the center flight line imagery for each hour of the ebb tidal cycle on the 6 April was rectified using a Bausch and Lomb ZT-4 zoom transfer scope at NASA/Langley Research Center. This rectified image of the thermal plume was traced on a line drawing of the inlet taken from the aerial photography for each hour of the tidal cycle to retain a common scale of 1:20,000.

The purpose of this portion of the study was to investigate the relationship of the visible suspended sediment or turbidity

plume with the sensed thermal plume. We expect that water directly related with the inlet storage system should be of a different temperature than the surrounding ocean water due to the differential heating effect on the shallower marsh area as opposed to the shelf water. The thermal scanner should sense this difference in temperature and delineate the marsh water accurately in a thermal plume. A comparison was therefore undertaken to see if the thermal imagery more accurately measured the change in marsh water flowing through the inlet than the visual color and color infrared imagery.

The outline of the area of the visual turbidity plume was superimposed on the thermal plume for each hour of the ebb tidal cycle photographed. It is interesting to note that the outline of the thermal plume corresponds very well with the visual turbidity plume.

The surface structure of the thermal plume is more complex than the visual turbidity plume. From Figure 1.11 a large body of relatively very warm water is visible to the east of the moderately warm inlet water which corresponds to the turbidity plume. This very warm water may be inlet water from a previous ebb tidal cycle from Wachapreague Inlet or from another nearby inlet. As the ebb tidal cycle progresses, several concentric bands develop with alternating moderate to cool water (Fig. 1.12). The very warm water to the east is still visible. The last two hours of ebb show the warmest water is now progressing from the inlet mouth (Fig. 1.13 and 1.14). A band of relatively cool water separates the warm

water from the moderately warm water. The finger-like structure of the eastern edge of the turbidity plume is somewhat reflected in the thermal plume on Figure 1.13, but there is no direct correlation on Figure 1.14, approximately one hour later.

The temperature differences on the thermal imagery are only relative. Ground truth data was taken by a single boat (see Welch and Haas, 1973). However, the boat was on a strict sampling schedule with specific stations over a large area of the mouth of the inlet, which was covered once over the four hours of the overflight. Simultaneous temperature measurements in different areas of the thermal plume were therefore not available.

In an effort to further define the thermal structure of the plume development, the enhanced thermal imagery was viewed on a spatial data systems 32 level color encoding densitometer, supplied by U. S. Geological Survey, Reston, Virginia. A Nikon FTN 35mm camera using kodak ektachrome x 135 film with a setting of f 3.5 at 1/4 sec was used to photograph each hour of the ebb tidal cycle on the visual display tube. The color slide was then rectified using tne Bausch and Lomb ZT-4 zoom transfer scope at NASA/Langley Research Center. This rectified image was then traced on a line drawing of the inlet from the aerial photography for each of the four hours of the tidal cycle studied at a common scale of 1:20,000.

The color encoded image produced the most detailed and complex structure of the thermal plume development. Figures 1.15 thru 1.18 show a black and white representation of the

color encoded image. Table 1.2 gives the code for the numbered contour lines which represent relative density values, which correspond to relative temperature values. Increasing numerical value represents cooler relative temperatures. As expected, the warmest water is in the marsh and inlet throat. The area of warm water suspected to be from the last tidal cycle is indicated by the number 15 contour line in Figure 1.15. A tongue of cooler oceanic water represented by the > number 30 contour can be seen migrating upcoast past the inlet, bisecting the warmer inlet thermal plume (Figures 1.15 to 1.18). The concentric bands of the inlet thermal plume become more pronounced and expand as the tidal cycle progresses, while the offshore thermal contours show a more complex pattern. The thermal plume reaches its longest area on Figure 1.18 where its outer boundary intersects the cooler tongue of oceanic water moving upcoast.

## Conclusion

Remote sensing techniques have been applied to the study on nearshore circulation in the vicinity of a natural inlet. Using sequential overflights on three days it was possible to photograph a complete tidal cycle. Using infrared color film it was possible to chart the growth and decay of a visual turbidity plume and calculate the change in area. The results show that the imagery allows estimation of turbidity depth once a storage volume graph has been developed for a particular inlet system.

Comparison of visual turbidity plume with thermal imagery indicates that the boundary of both the turbid water and temperature differences are similar. More detail into the structure of a plume is possible using thermal imagery. To best utilize this imagery for detailed structure color encoding with a densitometer is necessary. It is interesting to note the presence of banding structure on the thermal imagery. Visual inspection of the imagery shows alternating bands of relatively warmer and cooler water. However, color encoding indicates these bands are of progressively cooler temperatures seaward of the inlet.

TABLE 1.1

| Tide Stage | Time EST | Corrected Tidal Height | Plume Area From Aerial Photographs $Ft^2 \times 10^6$ | Plume Area From Aerial Photographs $\Delta Ft^2 \times 10^6$ | Plume Volume From Aerial Photographs $Ft^3 \times 10^6$ | Plume Volume From Aerial Photographs $\Delta Ft^3 \times 10^6$ | Wachapreague Inlet System Tidal Storage Volume ① $Ft^3 \times 10^6$ | Wachapreague Inlet System Tidal Storage Volume ① $\Delta Ft^3 \times 10^6$ | Plume Depth $\frac{\Delta Ft^3}{\Delta Ft^2}$ = Ft |
|---|---|---|---|---|---|---|---|---|---|
| | | | | | 6 April 1973 | | | | |
| Ebb | 1106 | 4.85 | 47.144 | | 645.272 | | 2,489.407 | | |
| | | | | + 46.115 | | +1,398.142 | | -1,059.322 | - 22.97 |
| Ebb | 1225 | 3.45 | 93.259 | | 2,043.414 | | 1,430.085 | | |
| | | | | + 33.911 | | +1,289.410 | | - 741.526 | - 21.87 |
| Ebb | 1346 | 2.10 | 127.170 | | 3,332.824 | | 688.559 | | |
| | | | | + 65.673 | | +2,576.816 | | - 406.073 | - 6.18 |
| Ebb | 1504 | 1.10 | 192.842 | | 5,909.630 | | 282.486 | | |
| | | | | | 7 August 1973 | | | | |
| Ebb | 0720 | 2.95 | 54.019 | | 829.781 | | 1,264.124 | | |
| | | | | + 3.360 | | + 88.378 | | - 105.932 | - 31.53 |
| Low | 0820 | 2.80 | 57.379 | | 918.159 | | 1,158.192 | | |
| | | | | - 2.614 | | - 11.006 | | + 49.435 | - 18.92 |
| Flood | 0910 | 2.85 | 54.765 | | 930.152 | | 1.207.627 | | |
| | | | | + 2.505 | | + 53.300 | | + 222.458 | + 88.81 |
| Flood | 1000 | 3.25 | 57.270 | | 883.452 | | 1,430.085 | | |
| | | | | - 16.530 | | - 341.471 | | + 423.729 | - 25.63 |
| Flood | 1058 | 3.90 | 40.740 | | 541.981 | | 1,853.814 | | |
| | | | | | 17 November 1973 | | | | |
| Flood | 1033 | 2.0 | | | | | 670.90 | | |
| | | | | | | | | + 423.73 | |
| Flood | 1124 | 2.7 | Data Not | Data Not | Data Not | Data Not | 1,094.63 | | Data Not |
| | | | | | | | | + 434.35 | |
| Flood | 1248 | 3.4 | Available | Available | Available | Available | 1,518.36 | | Available |
| | | | | | | | | + 70.62 | |
| High | 1342 | 3.5 | | | | | 1,588.98 | | |
| | | | | | | | | - 176.55 | |
| Ebb | 1435 | 3.2 | | | | | 1,412.43 | | |

①From Byrne and Penney, 1974.

Table 1.2

| Color Code \ Time of Imagery (EST) | 1106 | 1225 | 1346 | 1504 | Color | |
|---|---|---|---|---|---|---|
| 1 | | | | | | |
| 2 | | | | | Yellow | |
| 3 | | | | | | |
| 4 | | | | | | |
| 5 | | | | | | |
| 6 | | | | | Cyan | |
| 7 | x | | | | | |
| 8 | x | | | | | |
| 9 | | x | x | x | | |
| 10 | | x | x | x | Green | |
| 11 | x | x | x | x | | |
| 12 | x | x | x | x | | |
| 13 | x | x | x | x | | |
| 14 | | x | x | x | Orange | |
| 15 | x | x | x | x | | |
| 16 | | x | x | x | | |
| 17 | | x | x | x | | |
| 18 | | x | x | x | Magenta | |
| 19 | | x | x | x | | |
| 20 | | x | x | x | | |
| 21 | | x | x | x | | |
| 22 | | x | x | x | Violet | |
| 23 | x | x | x | x | | |
| 24 | x | x | x | x | | |
| 25 | x | x | x | x | | |
| 26 | x | x | x | x | Red | |
| 27 | x | x | x | x | | |
| 28 | x | x | x | x | | |
| 29 | x | x | x | x | | |
| 30 | x | x | x | x | Blue | |
| 31 | | x | x | x | | |
| 32 | | x | x | x | | |

Relative Decreasing Density Interpreted as Decreasing Temperature

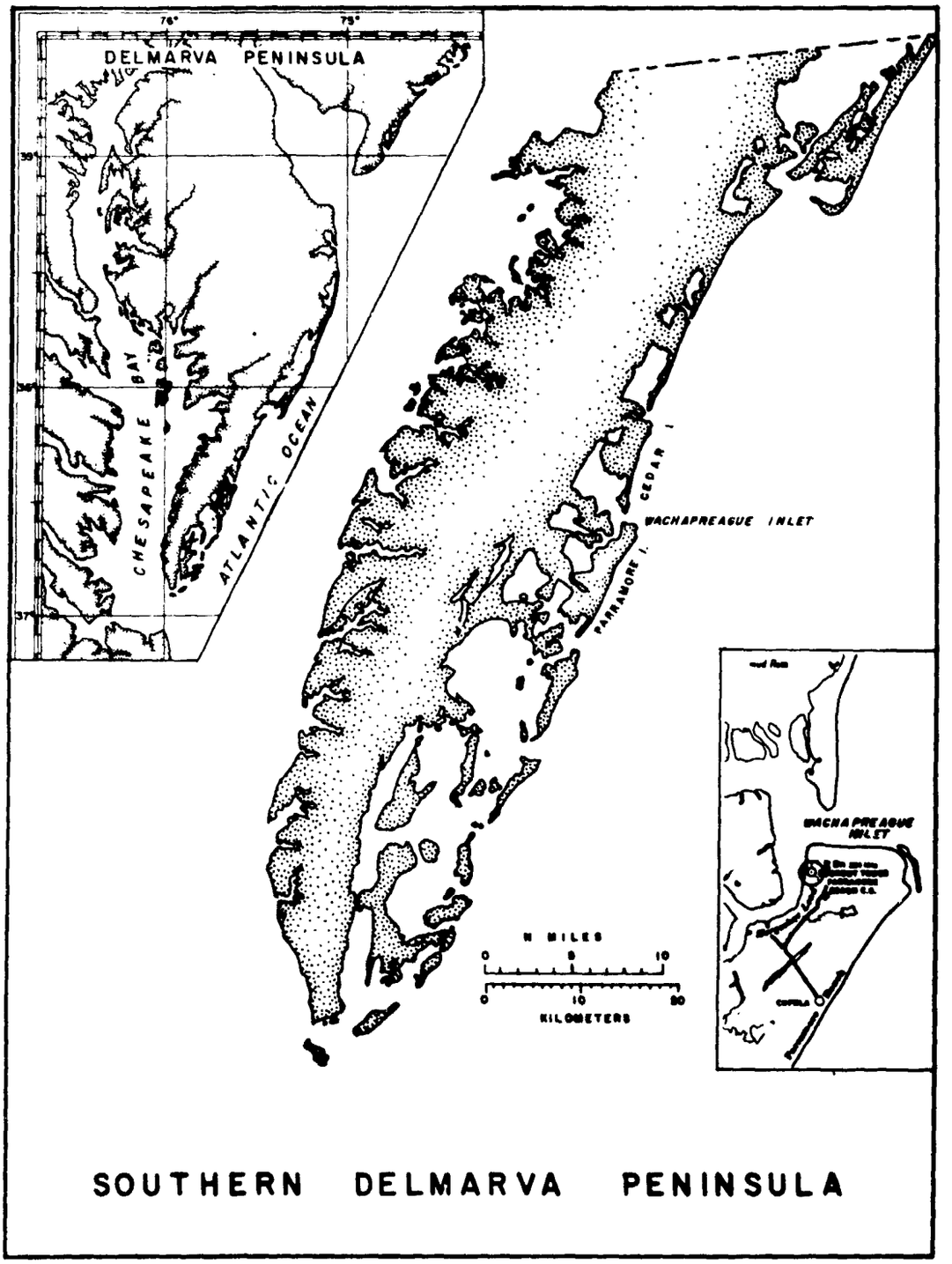


Figure 1.1. Location Map.

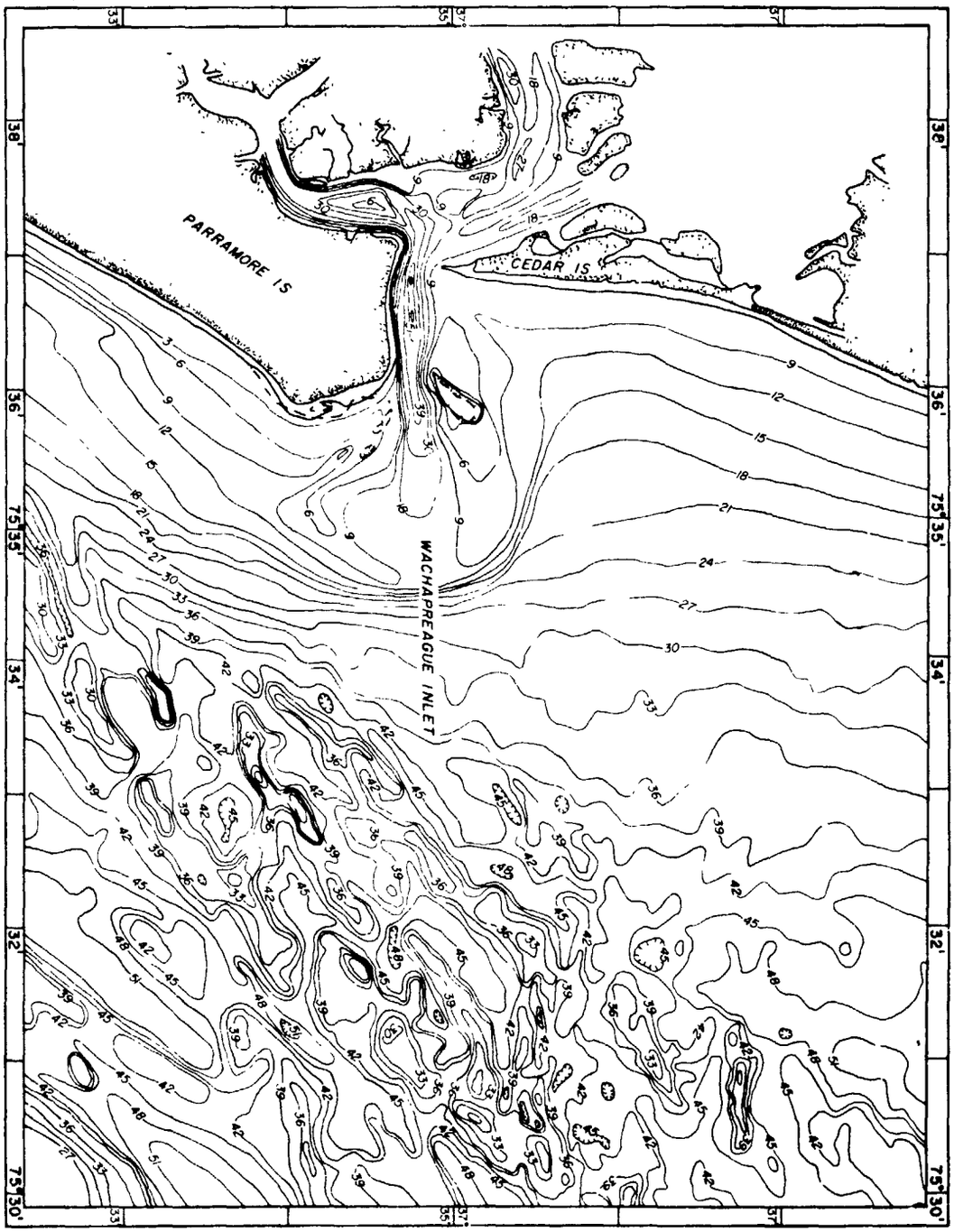


Figure 1.2. Bathymetry Map.

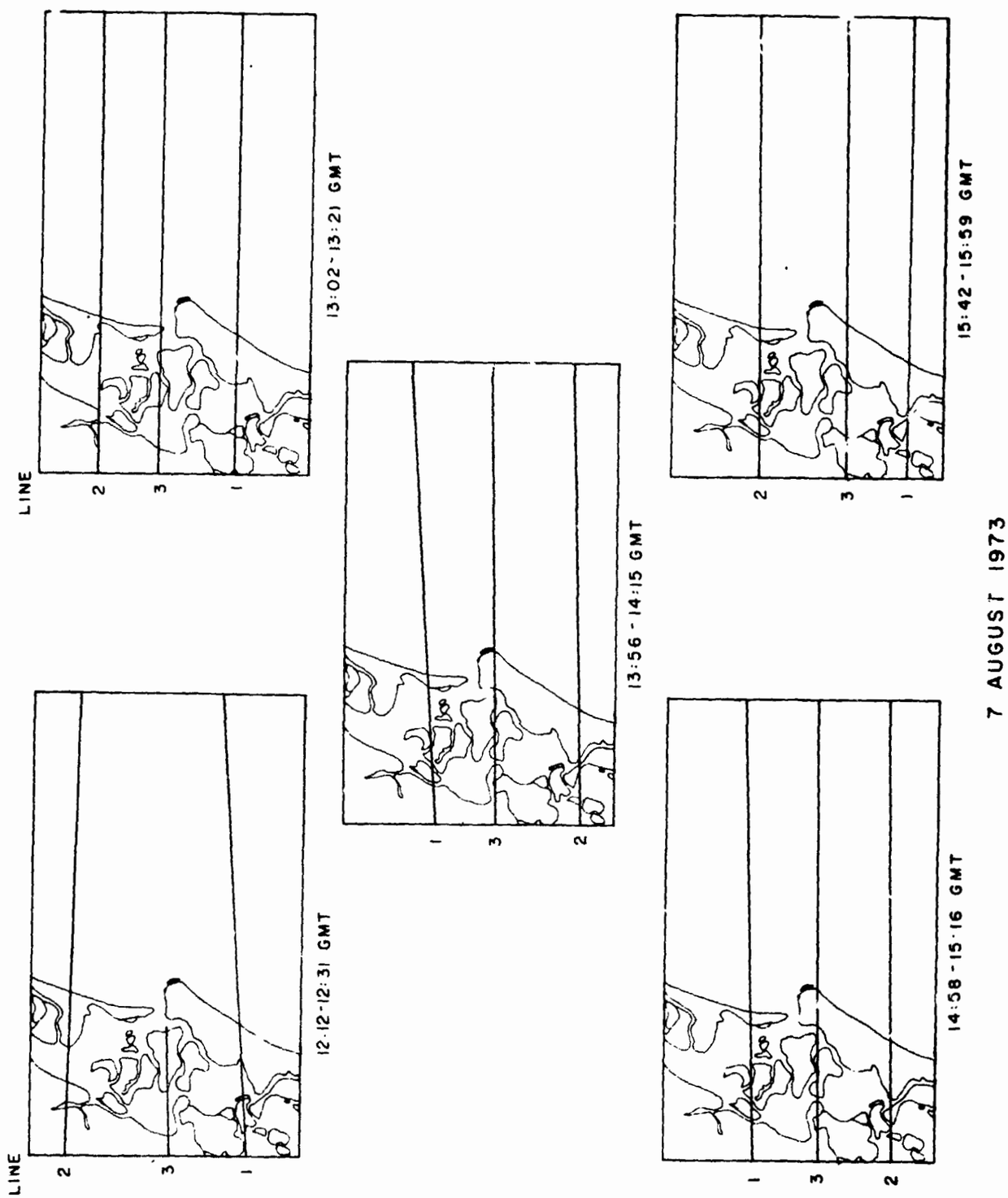


Figure 1.3. Flight Lines, 6 April.

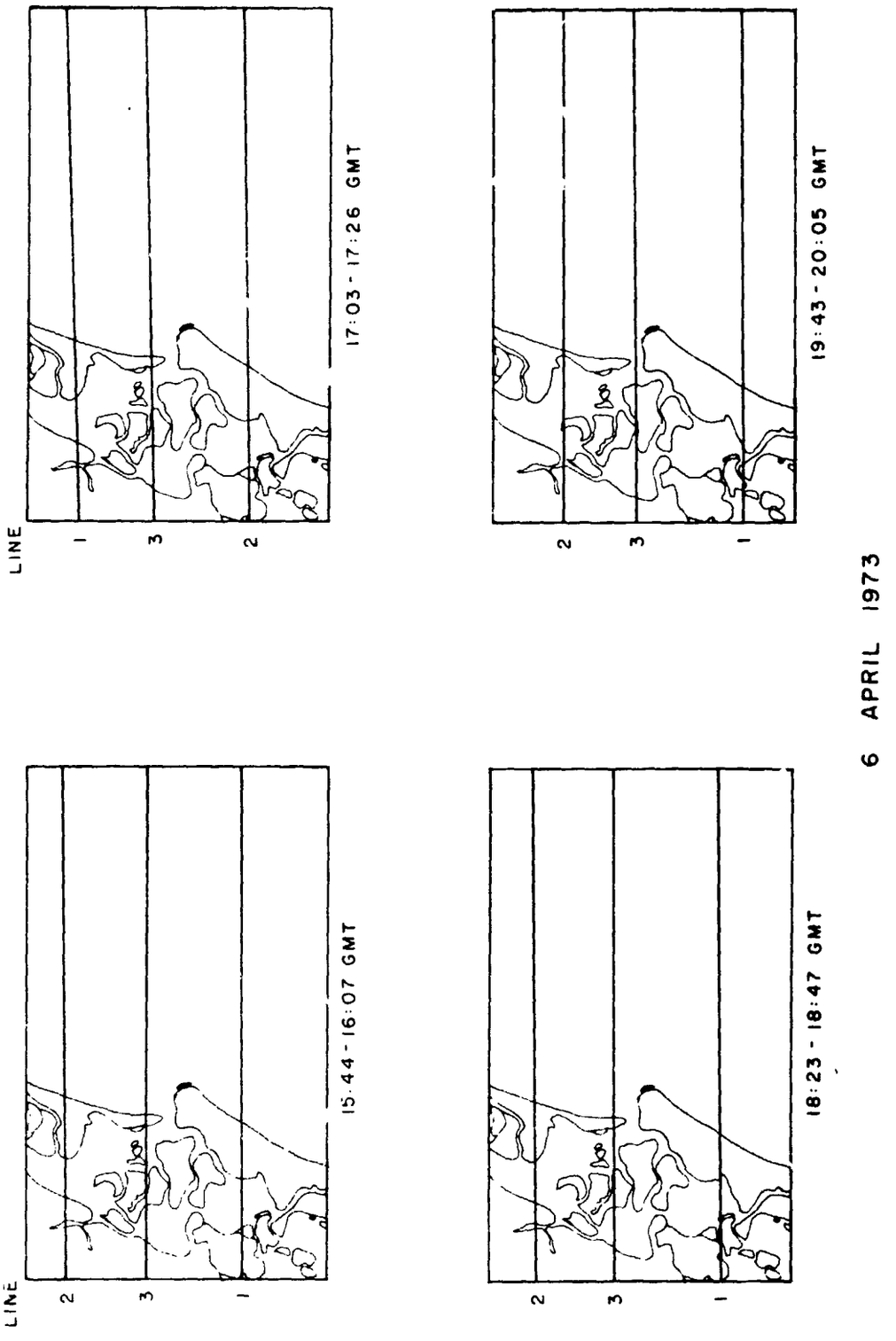


Figure 1.4. Flight Lines, 7 August.

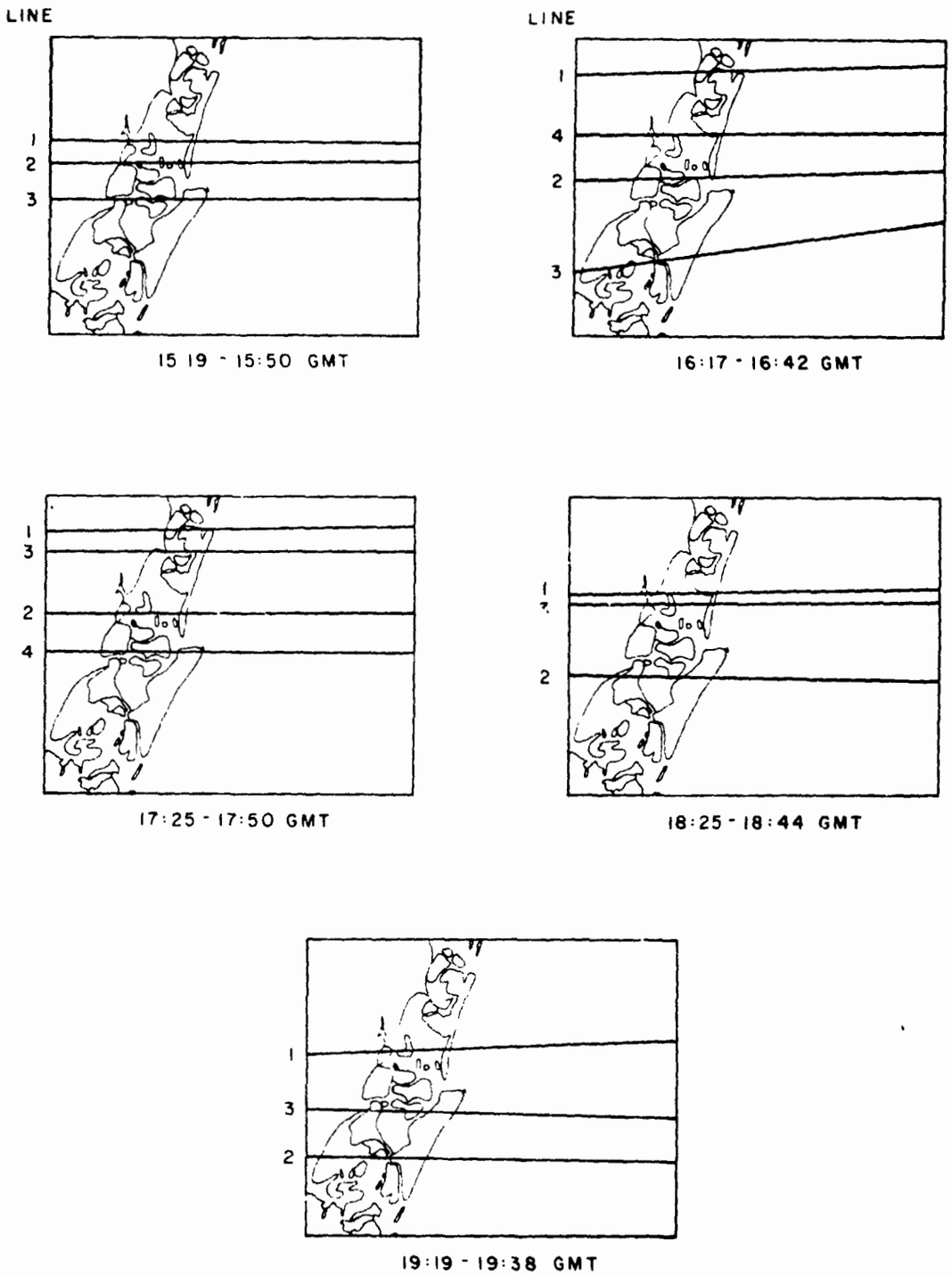


17 NOVEMBER 1973

Figure 1.5. Flight Lines, 17 November.

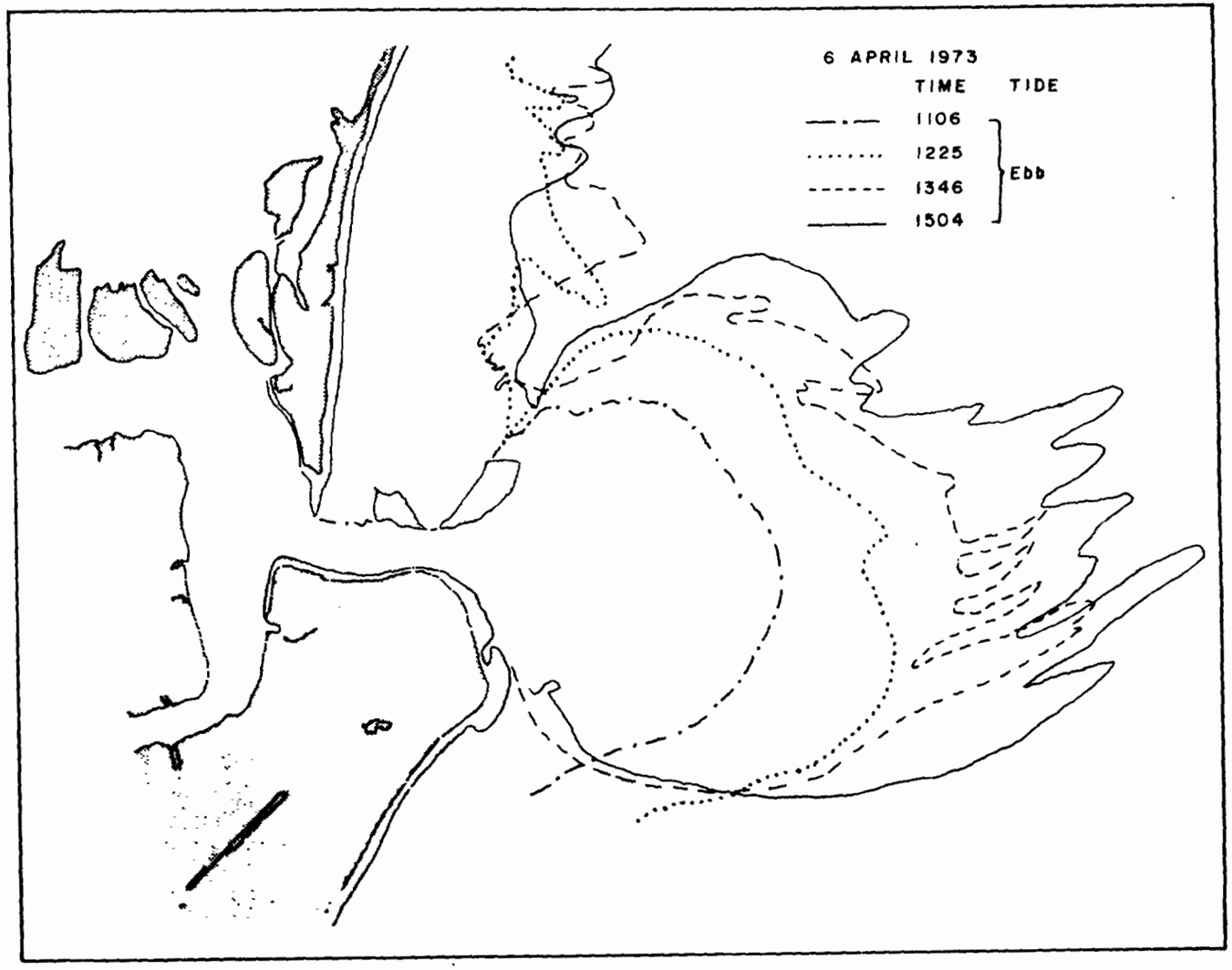


Figure 1.6. Growth Sequences of Suspended Sediment Plume on 6 April 1973, during Ebb Tidal Cycle (from Aerial Photography).

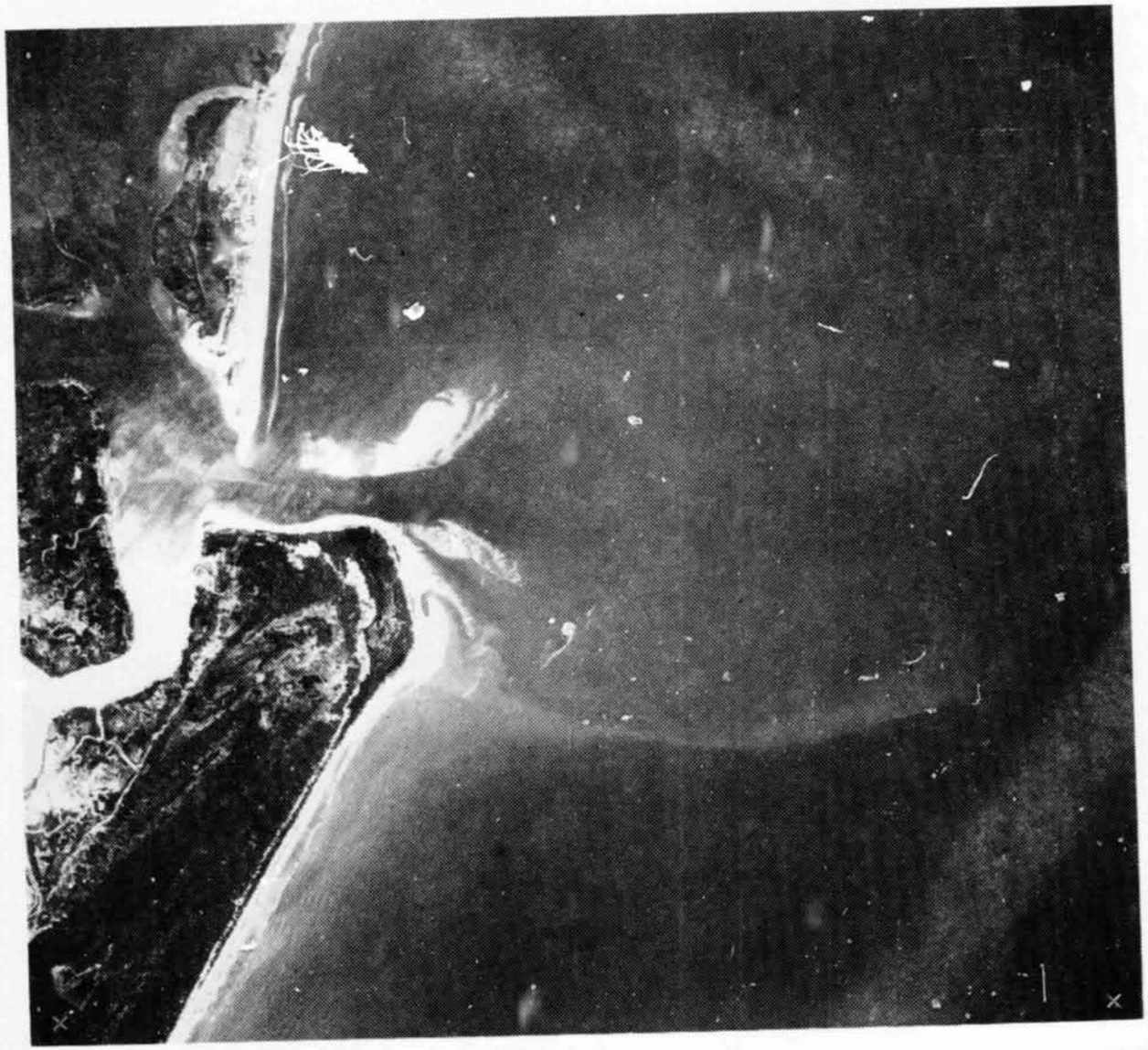

Figure 1.7. Black and White Print from Color Infrared Aerial Photograph of Wachapreague Inlet showing Suspended Sediment Plume during Ebb Tide, 6 April 1973, 1346 EST.

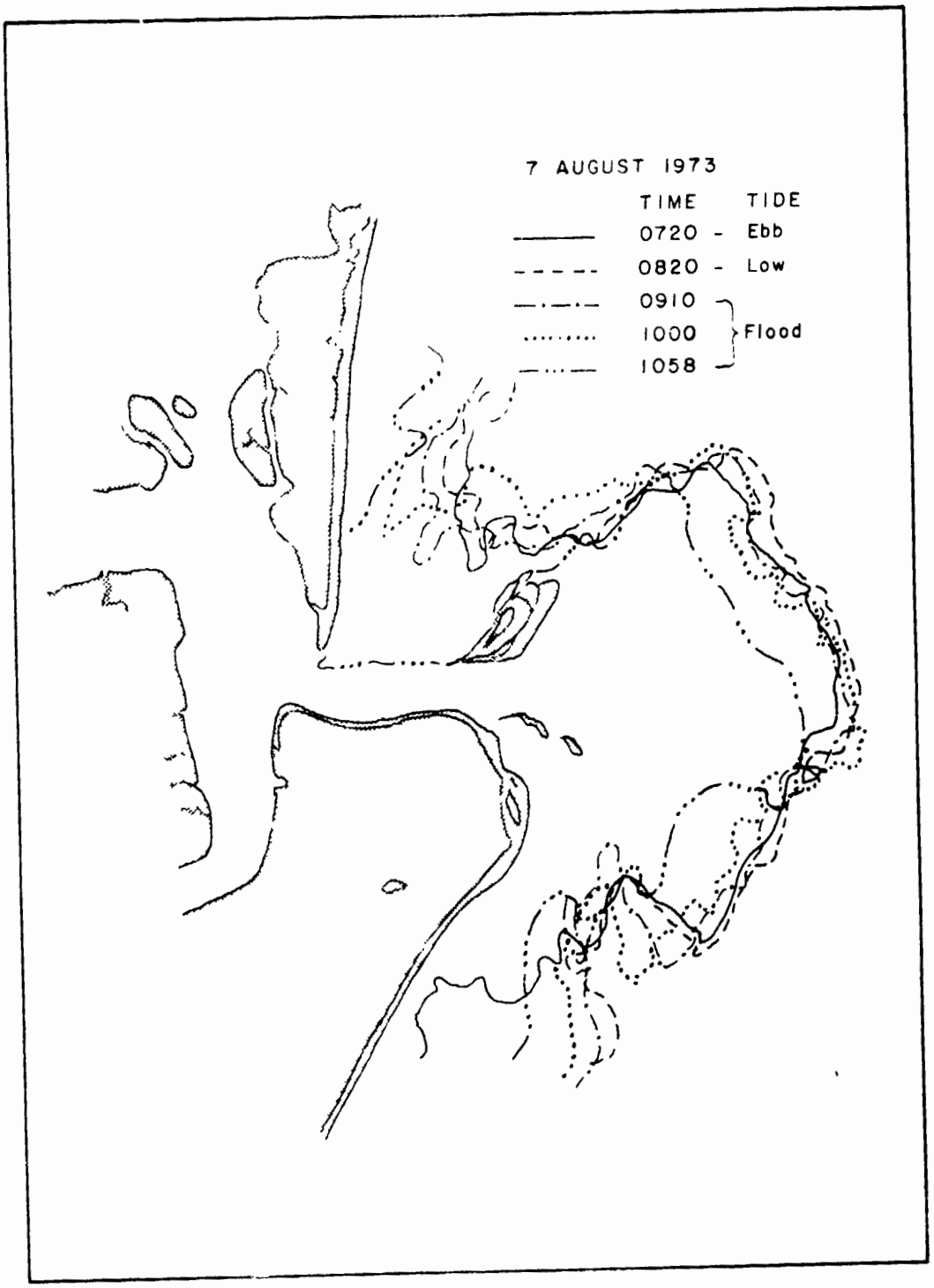


Figure 1.8. Change in Suspended Sediment Plume on 7 August 1973, during Last Stage of Ebb, Low and First Half of Flood Tide (from Aerial Photography).

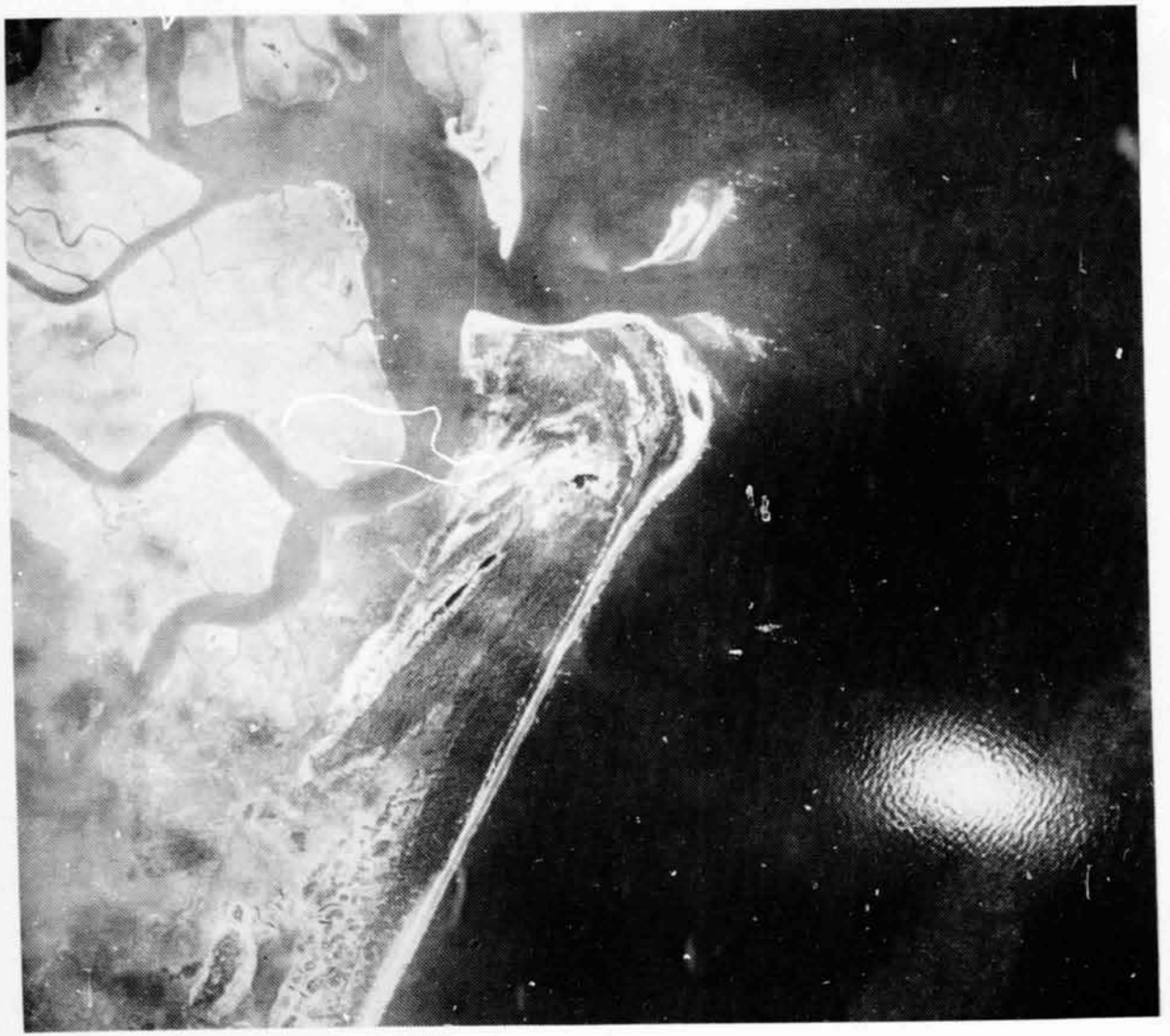

Figure 1.9. Black and White Print from Color Infrared Aerial Photograph of Wachapreague Inlet showing Suspended Sediment Plume during Flood Tide, 7 August 1973, 1000 EST.

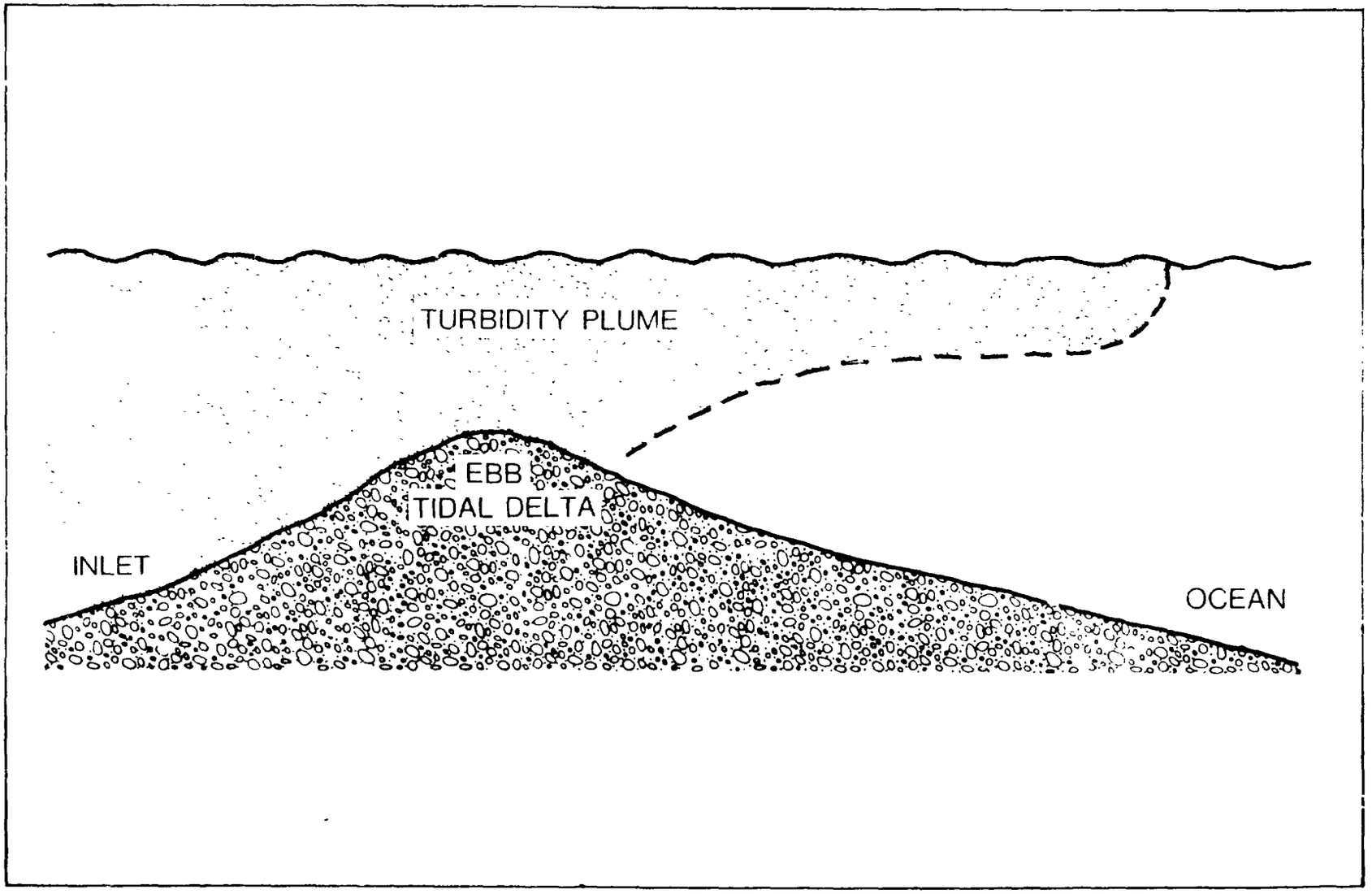


Figure 1.10. Hypothetical Cross-Sectional Structure of Turbidity Plume over Ebb Tidal Delta.

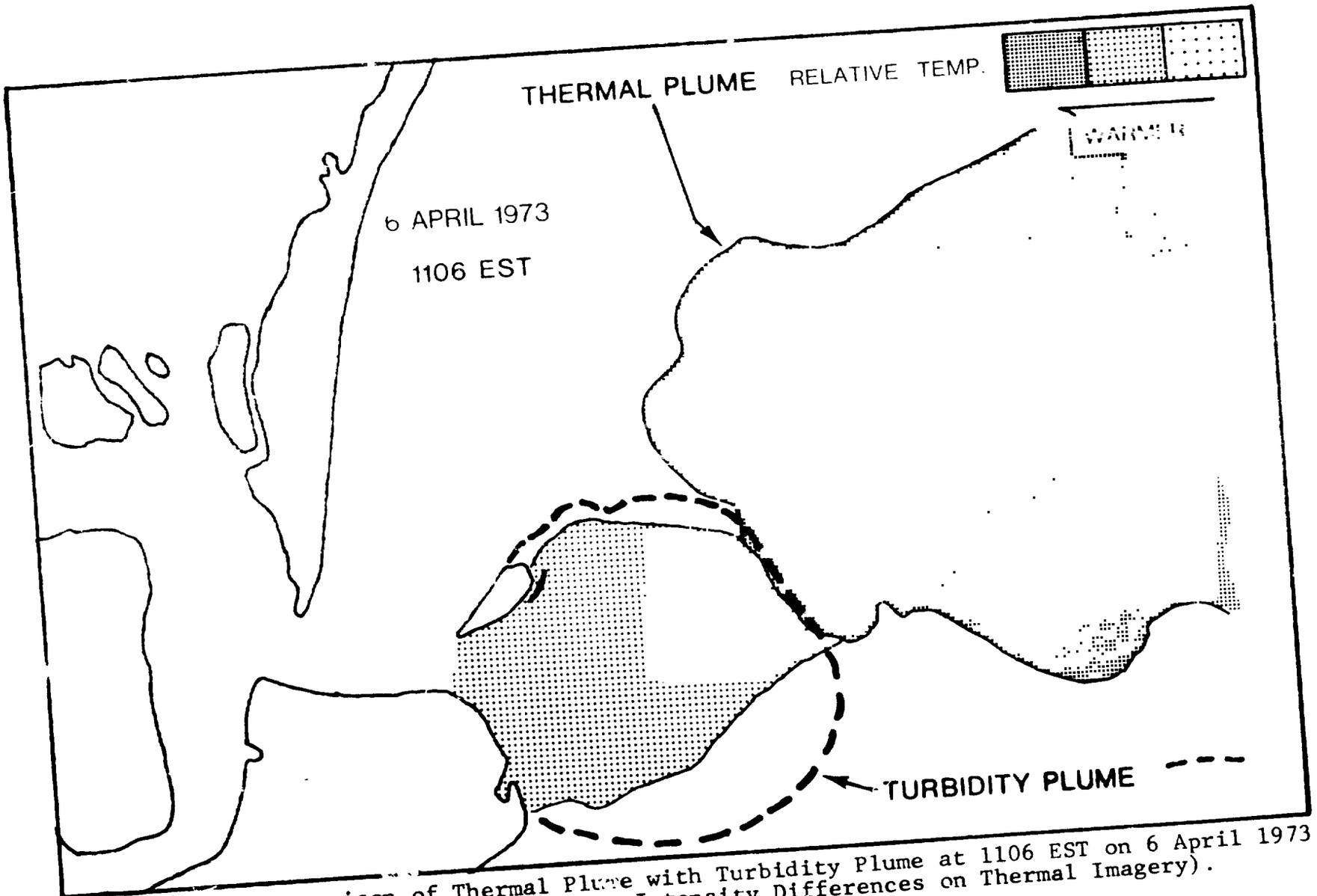


Figure 1.11. Comparison of Thermal Plume with Turbidity Plume at 1106 EST on 6 April 1973. (Relative Temperature from Intensity Differences on Thermal Imagery).

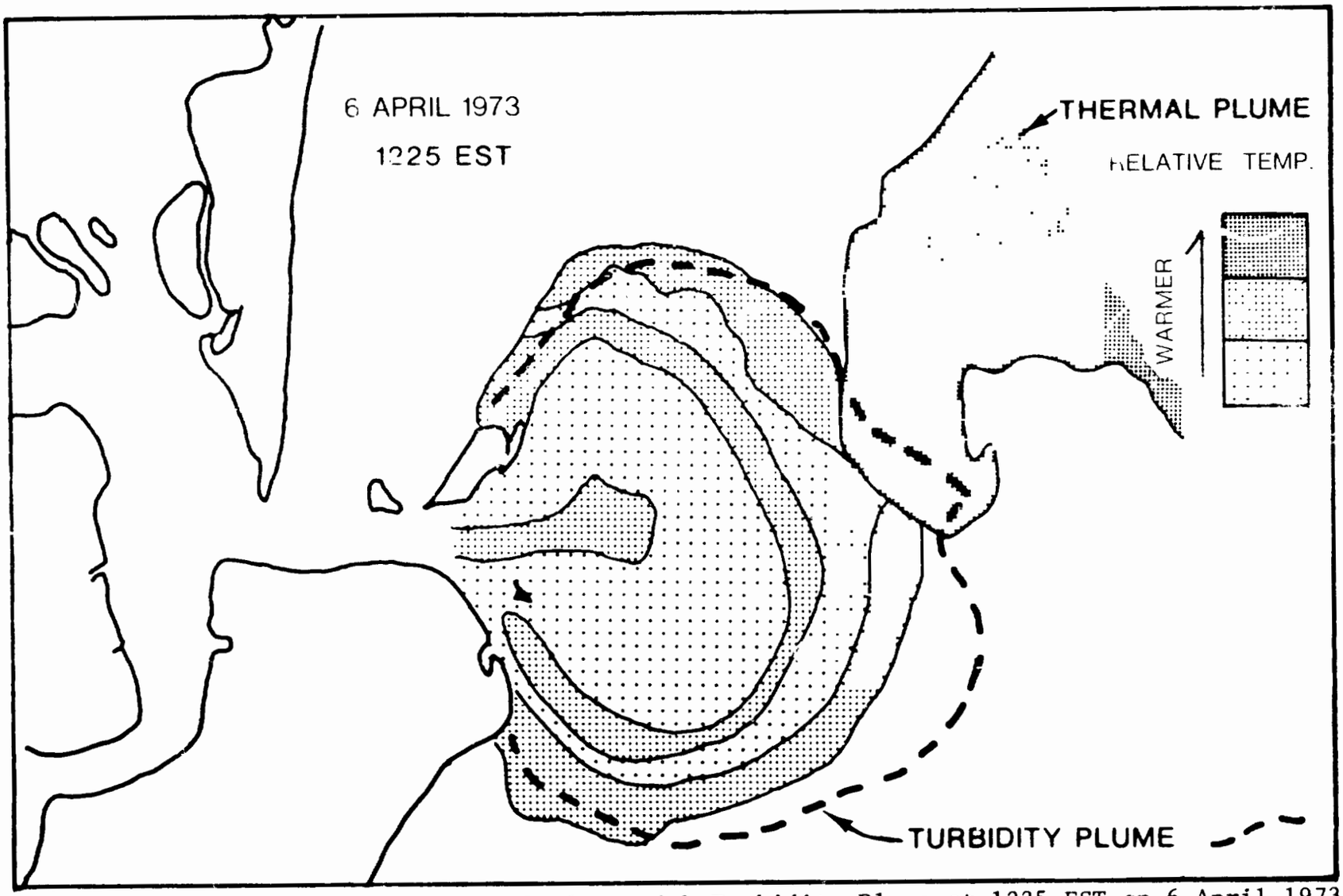


Figure 1.12. Comparison of Thermal Plume with Turbidity Plume at 1225 EST on 6 April 1973. (Relative Temperature from Intensity Differences on Thermal Imagery).

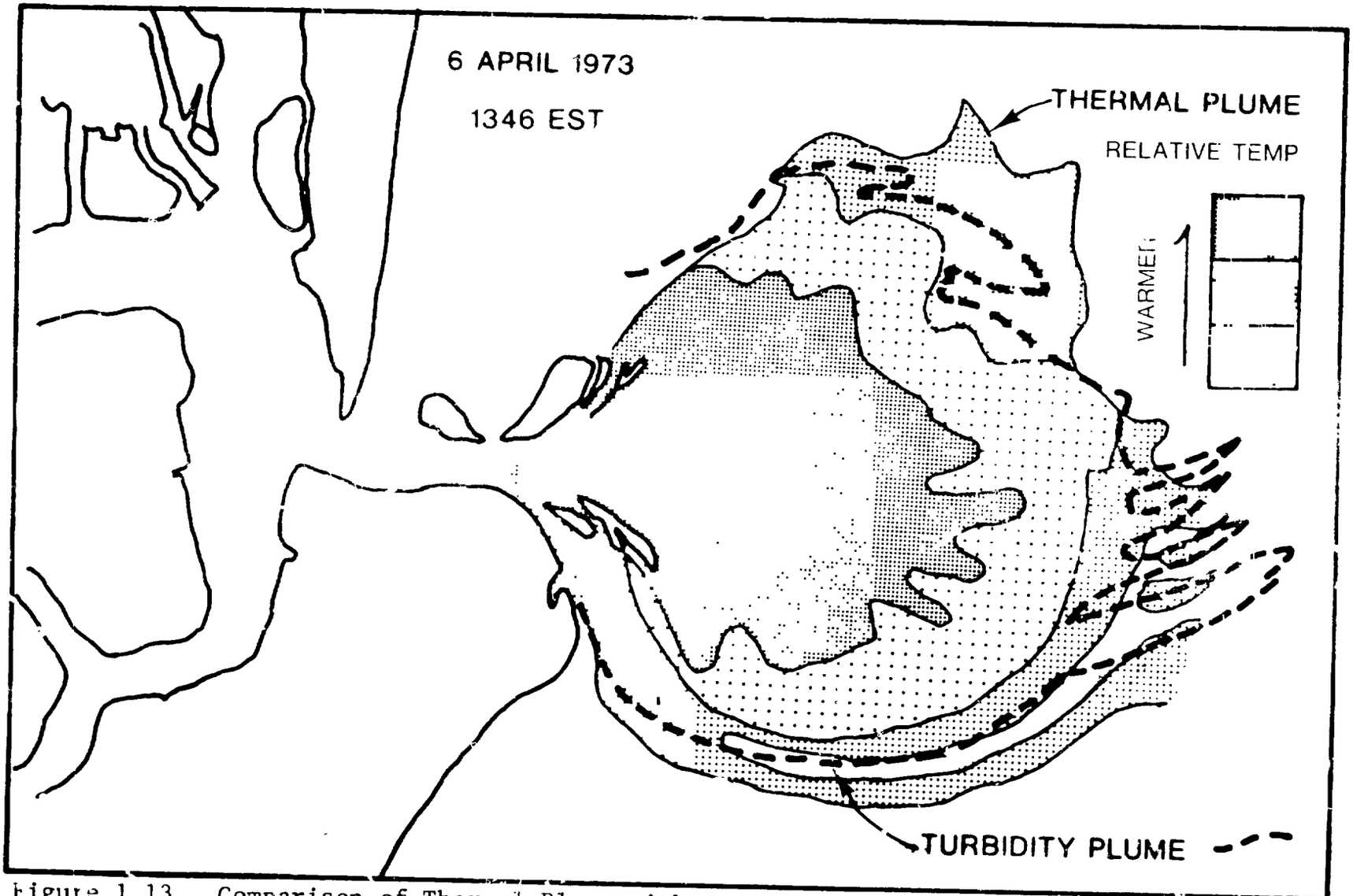


Figure 1.13. Comparison of Thermal Plume with Turbidity Plume at 1346 EST on 6 April 1973. (Relative Temperature from Intensity Differences on Thermal Imagery).

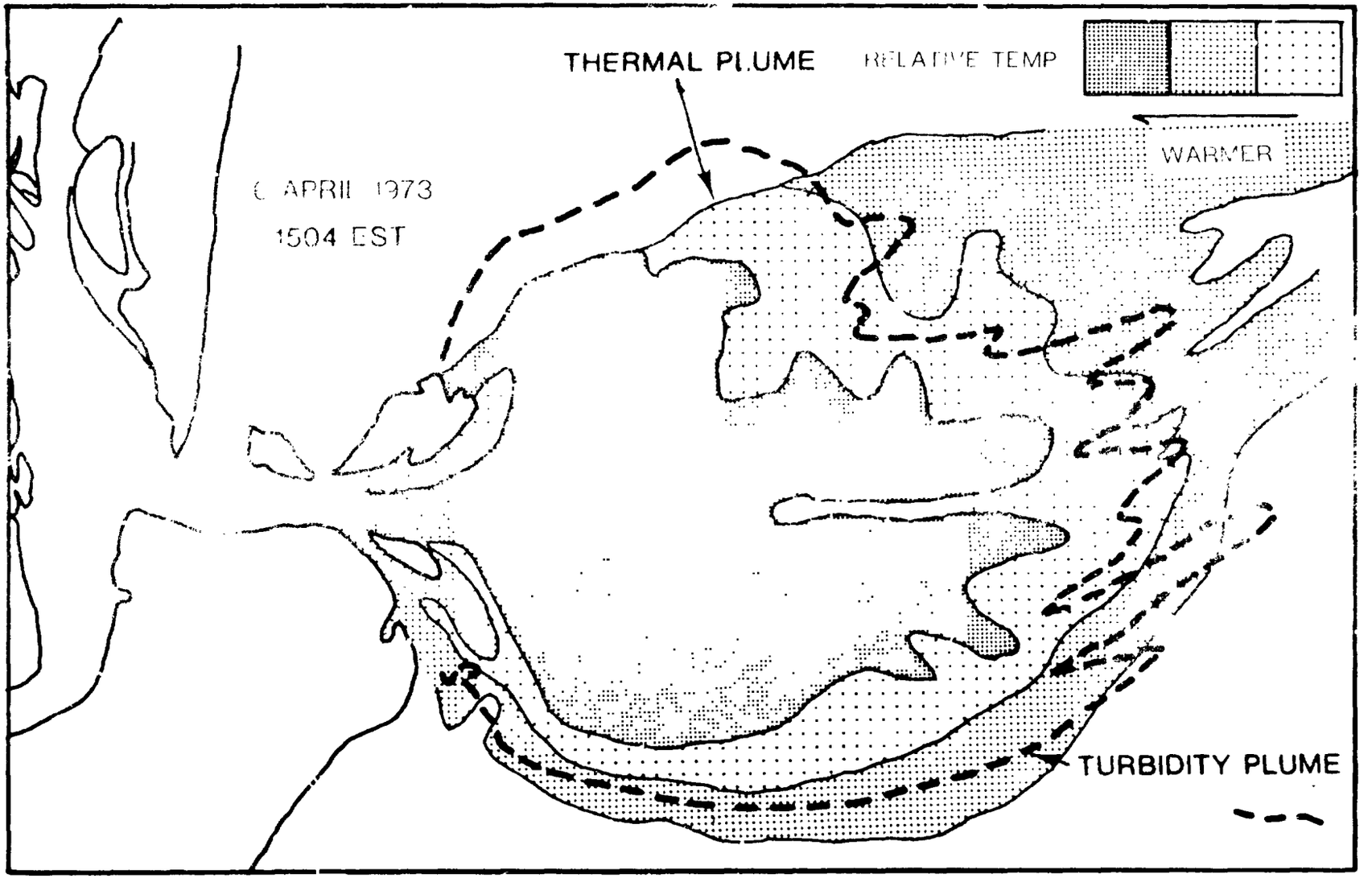


Figure 1 14. Comparison of Thermal Plume with Turbidity Plume at 1504 EST on 6 April 1973. (Relative Temperature from Intensity Differences on Thermal Imagery).

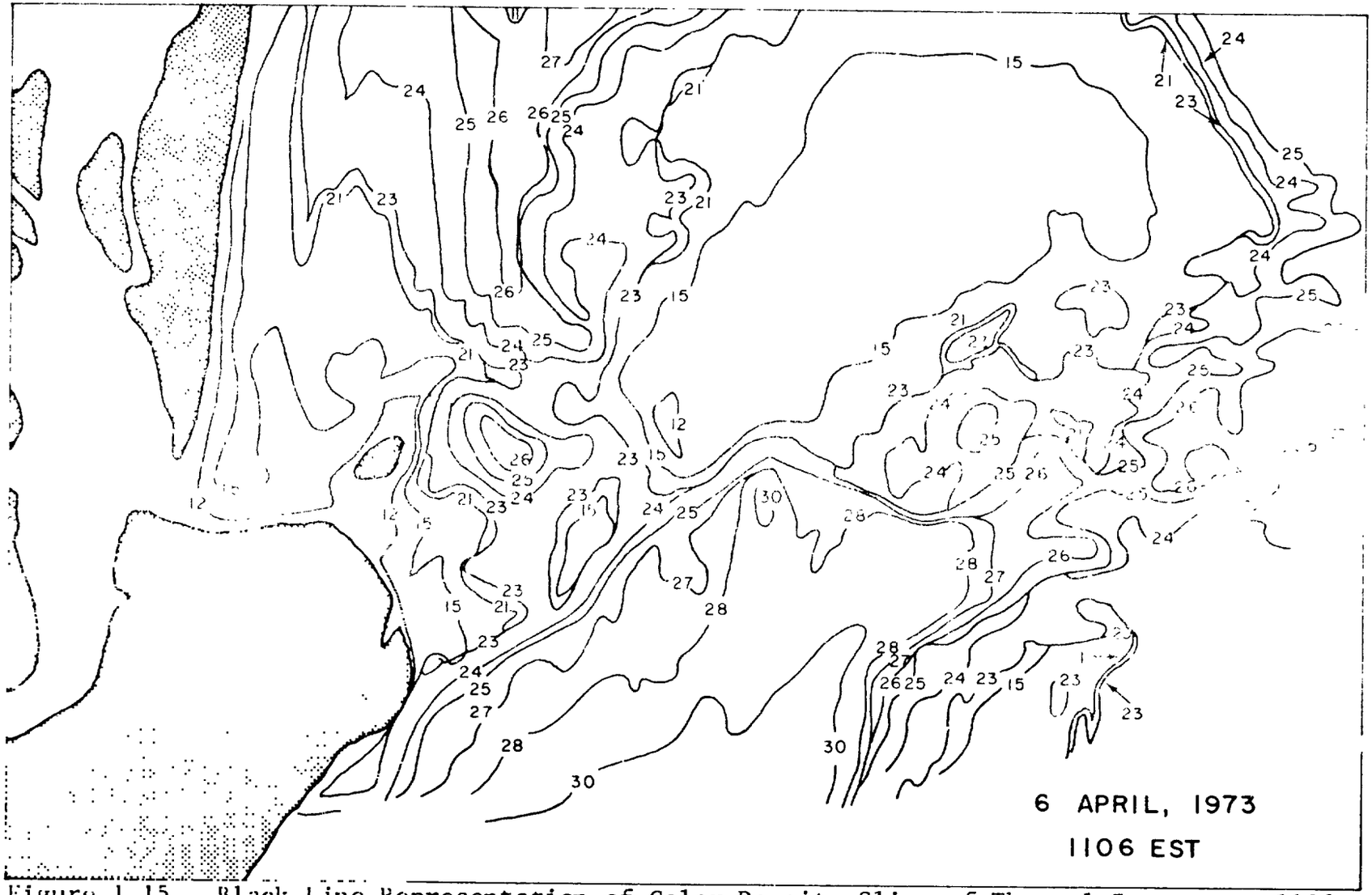


Figure 1.15. Black Line Representation of Color Density Slice of Thermal Imagery at 1106 EST on 6 April 1973. (See Table 1.2 for Explanation of Color Code Numbered Contour Lines Represent Relative Temperatures).

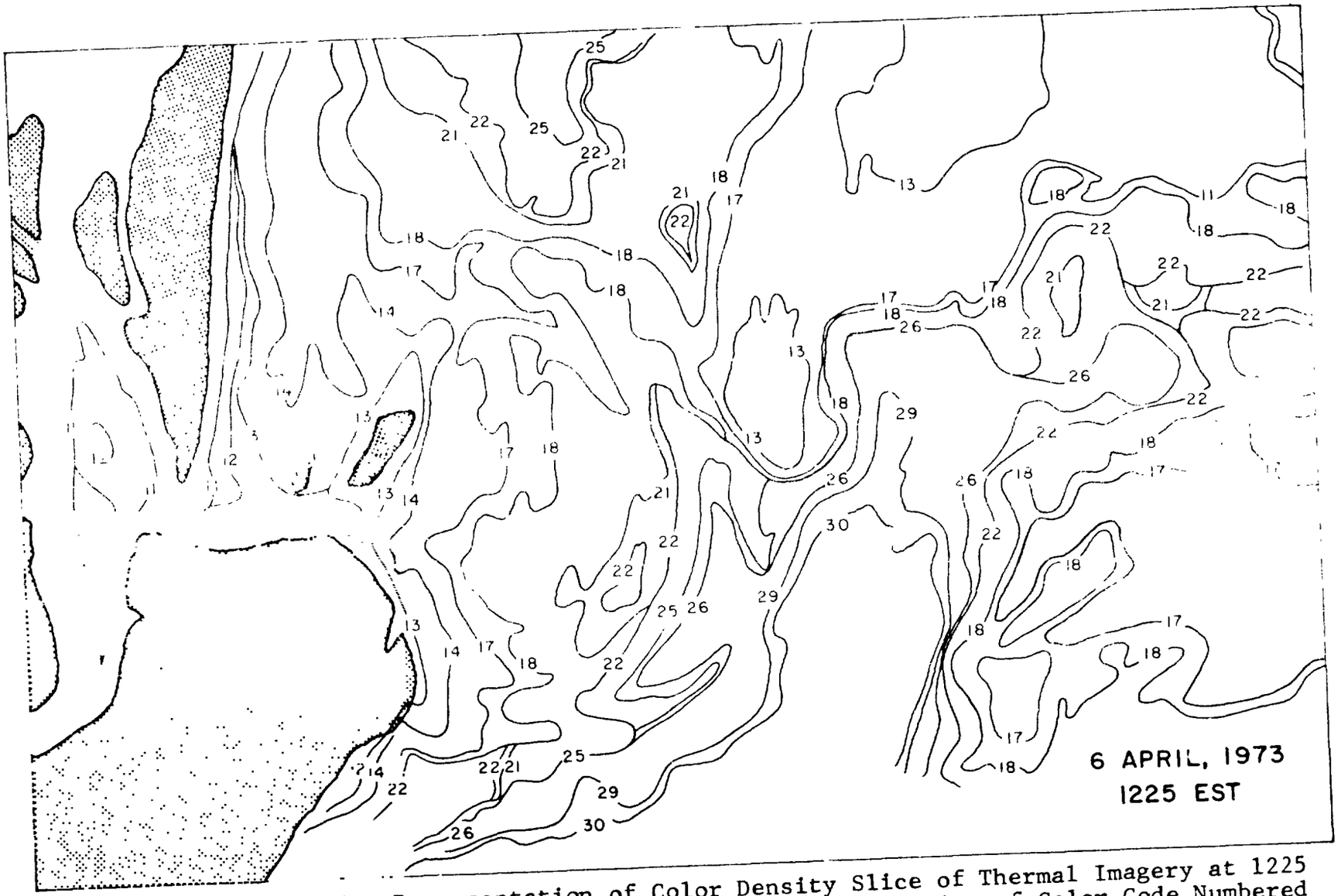


Figure 1.16. Black Line Representation of Color Density Slice of Thermal Imagery at 1225 EST on 6 April 1973. (See Table 1.2 for Explanation of Color Code Numbered Contour Lines Represent Relative Temperatures).

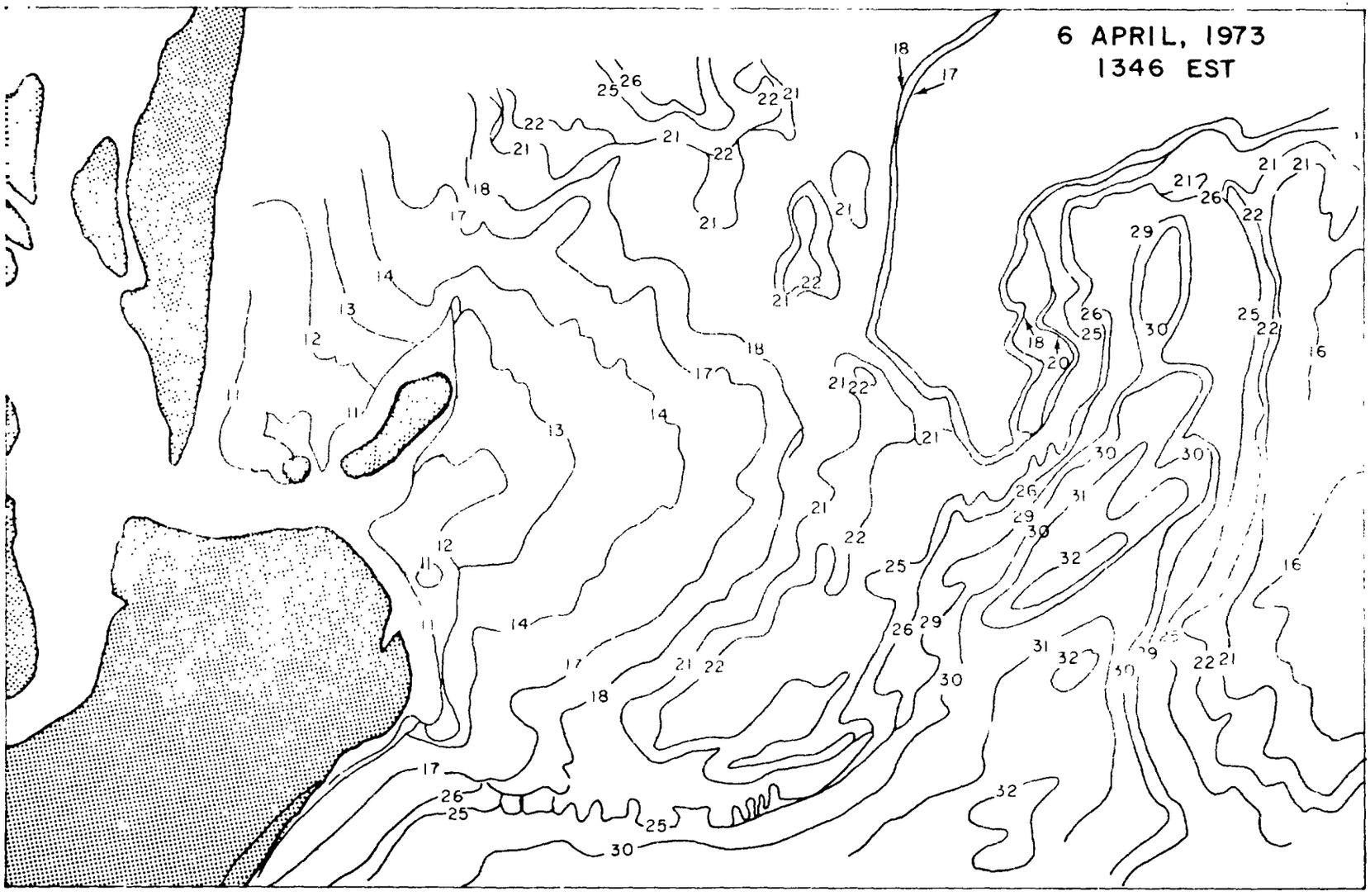


Figure 1.17. Black Line Representation of Color Density Slice of Thermal Imagery at 1346 EST on 6 April 1973. (See Table 1,2 for Explanation of Color Code Numbered Contour Lines Represent Relative Temperatures),

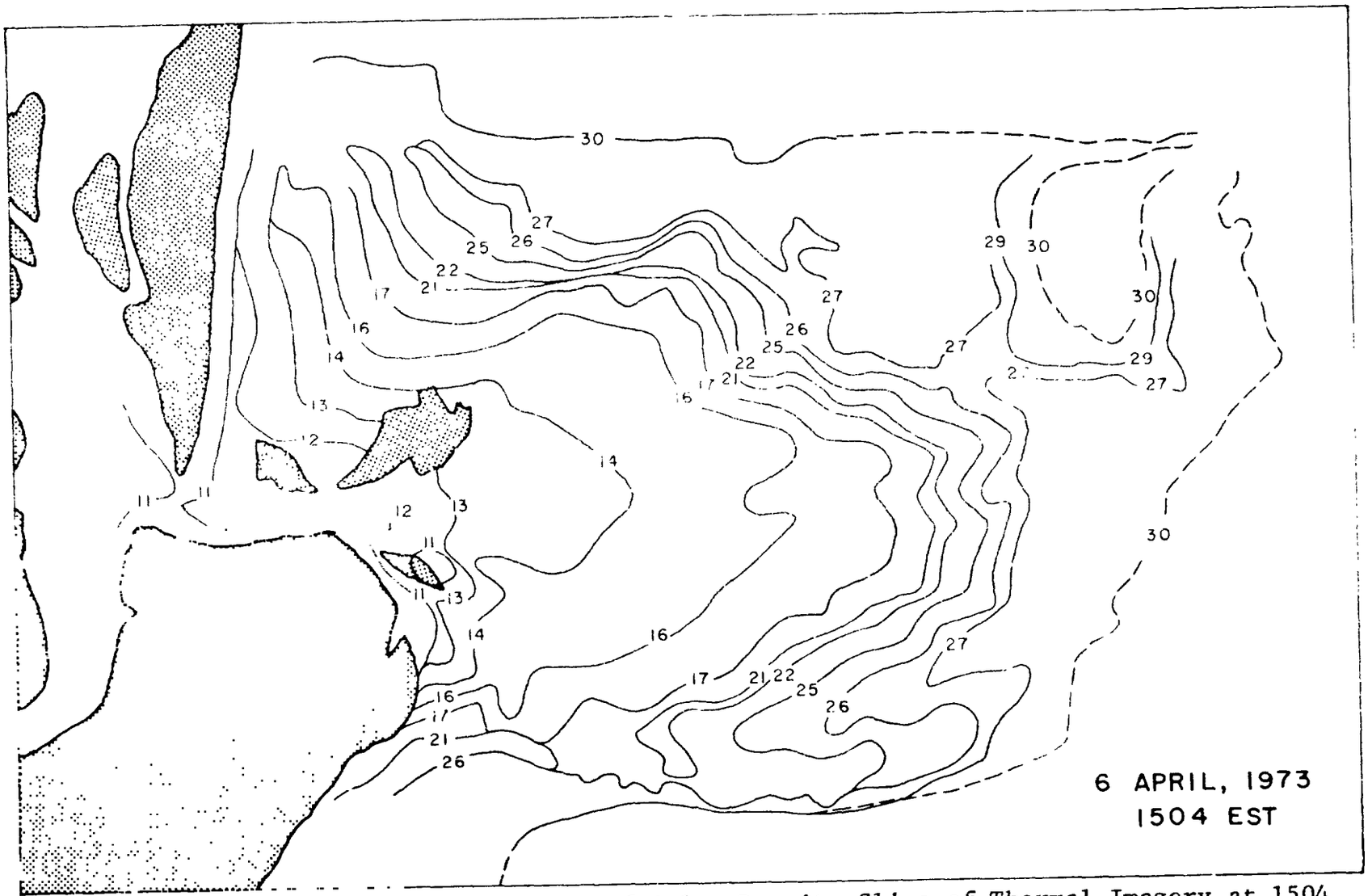


Figure 1.18. Black Line Representation of Color Density Slice of Thermal Imagery at 1504 EST on 6 April 1973. (See Table 1.2 for Explanation of Color Code Numbered Contour Lines Represent Relative Temperatures).

APPENDIX 2

# IDENTIFICATION OF INDICATORS OF BIOLOGICAL ACTIVITY

The second year of work under this contract witnessed the continuation and termination of the biological monitoring at Wachapreague Inlet on the Eastern Shore of Virginia. The primary objectives of this work remained the same: to measure a wide variety of biological and hydrographic indices in the marsh and nearshore waters (0-4 miles offshore) to determine which indices best characterize the respective water types, with the eventual goal of remote sensing those considered significant; to determine the direction and magnitude of the flux of biologically related materials (inorganic and fixed carbon) between the marsh and nearshore waters.

The seaside of Virginia's Eastern Shore is particularly well suited for a study of this nature. It contains $6.60 \times 10^4$ acres of salt marsh and $6.65 \times 10^4$ acres of tidal mud flats, 40 to 85 percent respectively of Virginia's totals (Wass and Wright, 1969) lying adjacent to, but separated from the coastal waters by a chain of barrier islands (Fig. 2.1). Interaction between the marsh and adjacent coastal waters normally occurs through well defined inlets that punctuate the coastline. One of these, Wachapreague Inlet, is of particular interest because of related hydrographic work at this inlet described elsewhere in this report.

The general technique utilized in this study was to measure a variety of biological and hydrographical indices at hourly intervals over a tidal cycle at fixed points near the Inlet and on transects extending from within the marsh to several miles offshore at selected times (usually slack tides) during a tidal cycle. Station designations are shown in figures 2.1, 2.2 and 2.3. All samples were taken at about one half meter depth.

The indices were measured and their method of measurement was as follows:

Water temperature was measured by stem thermometer.

Salinity was measured by an inductive salinometer.

Dissolved oxygen was measured by the azide Winkler titration.

The extinction coefficient (designated k and in terms of $m^{-1}$) is a measure of light attenuation through the water column and therefore, is a function of water turbidity. It was determined with a submersible lux meter in conjunction with a measure of incident light using the formula:

$$\frac{L}{L_o} = e^{-kz}$$

where: $L$ = light level at depth z in meters

$L_o$ = incident light level

$e$ = natural based logarithm

$k$ = extinction coefficient ($m^{-1}$)

Chlorophyll, a content of the water, was determined by fluorometric measurement (Turner model fluorometer) of 90%

acetone extracts of filtered water samples (100-250 ml filtered with Gelman type A glass fiber filters).

Potential primary productivity is a relative measure of carbon fixation by the phytoplankton and was determined by the rate of $^{14}C$ bicarbonate assimilation under controlled light and ambient temperature conditions.

Heterotrophic metabolism (termed Vmax) is a relative measure of the metabolic rate of the heterotrophic plankton (presumably bacteria) and was measured by the rate of $^{14}C$ glucose assimilation at various added substrate levels (37.5 to 375 $\mu g l^{-1}$).

Nutrients: particulate organic nitrogen, dissolved organic nitrogen, ammonia, nitrate, nitrite, reactive phosphate, dissolved organic carbon, particulate organic carbon and bicarbonate were measured with methods taken from Strickland and Parsons (1968).

## Results

On April 3, water samples were taken at stations X and Y at hourly intervals over the ebb tide and the first three hours of flood (Table 2.1). The temperature showed a steady increase and decrease during the ebb and flood tides respectively, with a slack tide difference of nearly 4°C. Salinity decreased and dissolved oxygen increased with the ebb tide although slack tide differences were not large, especially for dissolved oxygen. Both chlorophyll and Vmax appeared to reach maximum values at mid-ebb and mid-flood with low values at times of slack tides. Primary productivity was not measured.

On April 6, sampling was coordinated with a NASA/Houston overflight of Wachapreague Inlet. During the ebb tide, samples were taken near stations X and Y at twenty minute intervals. Concurrently a boat took a total of thirty samples in a repeating pattern offshore (Fig. 2.2). The position of the boat at the time of each sample was determined from the overflight photographs.

Temperature and salinity values for stations X and Y were quite similar (Table 2.2). The temperature increased an average of 3.5°C and salinity decreased about 1% over the course of the ebb tide. Dissolved oxygens at stations X and Y showed no particular trend and varied at both stations over a range of 2 $mgl^{-1}$. Chlorophyll values at station Y were greater and varied over a wider range than at X but in neither case did they display any particular trend over the ebb tide.

Of the thirty offshore water samples obtained on April 6, six were determined not to be in the turbidity plume and twelve to be in the turbidity plume (Table 2.3). Average temperature in the plume was 1.25°C higher than out of the plume. The average salinity .33% lower in the plume than out of the plume. The "in plume" chlorophyll average of 4.14 $\mu gl^{-1}$ agrees closely with the average chlorophyll values of stations X and Y over the ebb tide. In light of the twofold greater chlorophyll values in the plume than out, one might have expected lower chlorophyll values at stations X and Y near the time of high slack tide. Vmax values were three times greater in the plume than out of the plume (.53 vs .17 $\mu gl^{-1}hr^{-1}$), the latter values

rarely exceeding .2 $\mu g l^{-1} hr^{-1}$. Vmax was not measured at stations X and Y.

On May 30, stations X and Y were sampled hourly over a complete tidal cycle. In addition stations A and D were sampled at the approximate time of the three slack tides. Sampling on the morning of May 31 made up for heterotrophy samples lost on the previous day (Table 2.4).

A slack tide temperature range of 3.5°C was noted over the tidal cycle with the marsh waters warmer than the nearshore waters, resulting in increasing and decreasing temperature with ebb and flood tides respectively. Temperatures at station D were similar throughout the day (ca 19°C). Station A temperatures were higher especially at low slack when the tidal creek was nearly depleted of water.

Salinity values at X and Y ranged less than 0.3 ppt over the tidal cycle with the lower values near low slack. No particular trend was seen in dissolved oxygen values or extinction coefficients throughout the tidal cycle.

Chlorophyll values, similar at stations X and Y, decreased with the ebb tide and increased with the flood tide. This indication of higher chlorophyll levels offshore is not supported by the consistently low values ($<3.0 \mu g l^{-1}$) at station D on that day. Station A chlorophyll values approached the offshore values at high slack tides but were much greater at low slack.

Vmax values at stations X and Y increased with the ebb tide and decreased with the flood tide. Station D values were

uniformly low ($< .2\ \mu g l^{-1} hr^{-1}$). Station A values were relatively low at high slack and extremely high at low slack.

On May 31, we were able to sample inside and outside a foam line demarcating the offshore extent of the ebb tide turbidity plume. Vmax values were .73 and .13 in and out of the plume respectively, while extinction coefficients were 1.45 and .69 in and out respectively.

On July 2, a transect of four stations extending from the mouth of Wachapreague Inlet to 4 miles offshore (Fig. 2.2) was sampled at high slack, mid-ebb and low slack tides. Since the turbidity plume associated with the ebb tide was easily visible offshore, we were able to ascertain our sampling position relative to it.

Temperature values showed no consistent relationship with the plume, increasing in an offshore direction at high slack and decreasing offshore at low slack (Table 2.5). Dissolved oxygen values averaged .66 $mg l^{-1}$ higher out of the plume than in the plume. Extinction coefficients were consistently near 1.0 out of the plume and average 1.86 in the plume. The higher values (more turbid water) showed a steady outward progression with the plume.

Chlorophyll values were nearly the same in and out of the plume. Primary productivity values show little relationship to the offshore progression of the plume and little difference in and out of the plume.

Vmax values averaged four times greater in the plume than out of the plume and the increased values show a steady outward progression with the plume.

On July 3, stations X and Y were sampled over a tidal cycle and stations A and B were sampled near low and high slack tides.

The temperature showed a 4°C slack tide range with low values near high slack and high values near low slack. Dissolved oxygen values were higher at high slack and decreased at low slack with a range of ca 0.8 $mgl^{-1}$ over the day.

Extinction coefficients decreased with the high slack tide although the low values of about 1.0 associated with offshore waters on the previous day were not evident at the inlet.

Chlorophyll values, which showed no difference on the previous day in direct sampling in and out of the plume, and productivity both appeared to peak at noontime in association with the high slack tide.

Vmax values were high at low slack and low at high slack tides, in agreement with the previous day's results.

Sampling at station A near low slack again produced extremely high chlorophyll, productivity and heterotrophy values similar to the situation found in May. Concurrent sampling at station B resulted in values more closely aligned with the values from X and Y.

On September 25, we sampled at station Y over a tidal cycle (Table 2.7). Temperature and salinity were both slightly higher at low slack, but the slack tide ranges were quite small, 0.5°C and .21 ppt respectively. Levels of dissolved oxygen

were lower near low slack with a slack tide range of .8 $mgl^{-1}$. Extinction coefficients increased throughout the ebb tide, decreased with the first of flood then increased with the end of flood chlorophyll and primary productivity increased generally throughout the day. Vmax values ranged from .45 to 1.0 $\mu gl^{-1}hr^{-1}$ and showed no apparent trend over the tidal cycle.

On November 11 and 12, we utilized the R. V. Ridgely Warfield from Johns Hopkins University on a cruise along the seaside of Virginia's Eastern Shore. On November 11 we occupied six stations in a 2x3 grid directly offshore of Wachapreague Inlet (Fig. 2.2). These stations were sampled such that by visual observation, stations 1, 2 and 3 were beyond the influence of the low slack turbidity plume, station 4 was directly in the plume, station 5 on the southern edge of the plume and station 6 to the north of the plume.

The temperature of the water in the plume was 3.5°C cooler than outside. The salinity was lower by 0.6 ppt. Extinction coefficients averaged two times greater in the plume than out (1.66 vs .80). Chlorophyll values did not appear to change greatly relative to position in or out of the plume and productivity rates were not available due to improperly prepared $^{14}C$ bicarbonate. Vmax values at station were two times greater than at station 1, 2, or 3 (.160 vs .077 $\mu gl^{-1}hr^{-1}$).

On November 12, a series of stations were occupied on a transect extending from the southern tip of Assateague Island south to Wreck Island. The stations were positioned such that

samples were taken directly opposite the major inlets on the Eastern Shore and opposite the major barrier island (Fig. 2.1). We anticipated that by sampling in this manner the influence of the inlets on the nearshore zone could be discerned.

There were several deficiencies inherent in this sampling scheme. Low slack tide, when the greatest influence of marsh water might be expected offshore, was not until mid-afternoon. Therefore, our morning stations may not adequately reflect the full potential of this influence. The sampling was further complicated by our lack of experience in locating turbidity plumes at inlets other than Wachapreague Inlet. Station designations had to be supplied in advance and could not be altered en route even if turbid water was encountered opposite a particular inlet.

Water temperature was measured at frequent intervals as the boat was moving. It displayed a consistent 1.5°C drop opposite each of the major inlets. Salinity did not reflect the presence of the inlets and the range for all stations was only 0.5 ppt. Extinction coefficients ranged from .75 to 1.25 and the highest value was found opposite Wachapreague Inlet.

Chlorophyll values were very high opposite Assateague Island, by far the highest values not associated with sediments seen in the entire study. Chlorophyll dropped rather steadily as we moved south reaching a low point opposite Cedar Island. From this point south there was a general increase in values.

Vmax values were consistently higher opposite the major inlets. The highest value was found opposite Wachapreague Inlet.

Discussion

Of the seven biological and hydrographic indices routinely measured in this study, almost all exhibited strong gradients either over time or space on at least one visit to the Wachapreague area. Assuming that tidal transport was the primary factor contributing to these gradients suggests the existence of quantifiable differences between the marsh and nearshore waters and the possibility of net flux of materials through the inlet. It is apparent however that of the several types of measurements made over the course of a year some are more reliable than others to distinguish quantitatively between the marsh and nearshore waters.

Strong temperature gradients, often approaching 4°C in magnitude, generally existed between the marsh and nearshore waters. The smallest temperature gradient (.5°C) occurred on September 25. Although the marsh waters were generally warmer than the offshore waters, the November cruise indicates that at times the reverse may be true. It is significant that surface water temperatures are easy to remote sense and the application of this technique is illustrated elsewhere in this report.

The degree of asymmetry in sequential temperature measurements over a tidal cycle near the inlet may be a good indicator of the net exchange of marsh and offshore waters over a complete tidal cycle. A symmetrical temperature curve indicates that the water entering the inlet on a flood tide is the same water that existed on the previous or ensuing ebb tide. The data from May 30 serves as an illustration. During the ebb tide,

the temperatures at stations X and Y increased approximately linearly from 17 to 21°C. On the ensuing flood tide, the water temperature decreased to 20 degrees during the first two hours, then suddenly dropped 2°C within an hour indicating that in this instance more cooler nearshore water entered the inlet on the flood tide, then left the inlet on the previous ebb tide.

A problem with this analysis is that our sampling was restricted to the surface and this asymmetry may reflect a wind related anomaly that is limited to surface waters and not indicative of transport through the entire water column. However, a string of temperature sensors through the water column in the Inlet may indicate the extent to which net exchanges of water types occur on a given tidal cycle.

Variations in salinity, although consistent (the marsh waters being less saline than the nearshore waters), were of such small range (generally less than 1 ppt) as to be of little value as a water tracer. The small salinity gradient is primarily a result of the very limited freshwater input into the marsh area influenced by Wachapreague Inlet. The result is marsh salinities consistently near 30 ppt.

Dissolved oxygen values, like salinity, were generally consistent in their variation (marsh water had lower oxygen levels than nearshore) but exhibited very small overall range in their magnitude. Sampling near the surface in such well mixed waters, it is not surprising that the oxygen values showed so little variation and were probably close to saturation for the particular salinities and temperatures found. The

slightly decreased oxygen levels in the marsh waters may reflect the increased heterotrophic metabolism of those waters as indicated by the consistently higher Vmax values. Were it not for the nearly complete tidal mixing one might expect to find greatly reduced oxygen values back in the small marsh channels where heterotrophic metabolism is highest.

The extinction coefficient is a function not only of water turbidity but also of the sun angle and degree of surface reflectance. Consequently, although the marsh waters are obviously more turbid than the nearshore waters, under certain conditions this difference might not be reflected in higher extinction coefficients. For example, in May strong gradients were observed in temperature, Vmax and salinity over a tidal cycle indicating the increasing influence of marsh water near the inlet toward low slack tide. This condition was not reflected by increased extinction coefficients. This may be due to the fact that the time of low slack, when one would expect the most highly turbid water near the inlet (i.e. high extinction coefficients) coincides with the time of minimum sun angle (noontime) which would tend to decrease extinction coefficients by decreasing surface reflectance.

The most consistent differences in extinction coefficients are found when different water types are monitored over a short time span in an effort to eliminate varying sun angle and surface reflectance conditions as modifying influences. In those cases where this was done (May 31, July 2 and November 11) obvious differences in water turbidity were reflected in widely

divergent extinction coefficients.

Since water turbidity is one of the primary indices routinely monitored by remote sensing, it is apparent that a direct rather than indirect measure of water turbidity is preferable.

Variation in chlorophyll levels between the marsh and nearshore waters appear puzzling. At times, chlorophyll gradients were noted with sequential sampling near the inlet over a tidal cycle when no difference could be found in direct sampling in the marsh and nearshore waters (July 2 and 3). At other times, exactly the opposite was true (April 6). A possible explanation of this paradox may be found in the fact that phytoplankton are known to undergo daily rhythms in chlorophyll content. Given the fact that nearly all the tidal cycles monitored encompassed the twelve daylight hours, it would be difficult to determine if a noontime peak in chlorophyll was the result of a tidal excursion centered on midday or an endogenous rhythm in chlorophyll production keyed to daylight but unrelated to the tidal cycle.

It would appear, therefore, that comparable samples of marsh and nearshore waters closely spaced in time would most nearly reflect true differences that might exist. On two of the three occasions when this was accomplished (April 16, July 2 and November 11) no difference was discernible in the chlorophyll content of the two water types.

The relatively low chlorophyll levels as compared with the York River or Chesapeake Bay found throughout this study

(rarely greater than 10 $\mu g l^{-1}$ and generally close to 5 $\mu g l^{-1}$) are probably caused by several factors. The high salinity, high turbidity and well mixed nature of the marsh waters would all tend to inhibit a well developed phytoplankton community, even in the presence of adequate levels of nutrients.

The occasional high chlorophyll levels found at station A at low tide (May and July) when only a few centimeters of water remained in the creek probably reflect the presence of mud diatoms in the water sample. These benthic algae may be so dense at times that the mud surface appears to be covered with a yellow-brown slime and their contribution to marsh productivity may be significant. Concurrent sampling at station B on July 3 indicates that the high station A values on that day were restricted to that latter station.

In view of the foregoing discussion, it would appear that chlorophyll level per se is not a reliable indicator to distinguish between marsh and nearshore waters. Given the generally low levels of chlorophyll and the high turbidity, the ability to remotely sense surface chlorophyll levels would appear remote indeed.

The use of the rate of primary productivity as an indicator of water types suffers the same drawbacks as chlorophyll. Even when productivity is measured under constant light conditions as we did, the rate undergoes a diurnal rhythm depending on the time of day the sample is taken. Our experience in the York River indicates that mid-morning and mid-afternoon rates are highest separated by a noonday "slump".

With our sampling method, it is impossible to distinguish between variations in primary productivity caused by diurnal rhythms and those caused by tidal transport.

Variations in heterotrophic metabolism as reflected in Vmax values appeared to be quite consistent. Marsh waters had higher values than nearshore waters and this difference was reflected consistently whether measurements were made over time at a fixed point or over space at a fixed time. September 25 was the only instance when this pattern was not detected.

The extremely high Vmax values found at station A at low tide (May and July) were probably caused by the inclusion of abnormal amounts of sediment in the water sample and reflect what may be a direct cause and effect relationship, that is the high Vmax values of the marsh waters may result from their increased sediment and detritus load with their accompanying bacterial flora. If this were the case, one might expect a strong relationship between extinction coefficients (as a measure of turbidity) and Vmax. In one instance, there appears to be a strong direct correlation between the two values (Table 2.10). In other cases the correlation is not so strong. In view of the inadequacy of the extinction coefficient as a true measure of turbidity, these correlations would probably be enhanced by more exact measure of turbidity. If this were the case, then in this particular instance, variations in heterotrophic metabolism could be remotely sensed by their quantifiable association with turbidity.

Although it was our original intention to measure nutrient levels in all of the water samples, difficulties in having them analyzed have delayed this possibility. The samples are still in cold storage and we anticipate eventually having the results.

During the second year of this study it became apparent that with the capabilities at our disposal we would be unable to make sufficient kinds or numbers of measurements to adequately estimate the flux of material through Wachapreague Inlet. However, based on the knowledge and experience gained through this project, a proposal to an alternative funding agency focusing solely on this question is presently in preparation.

With the termination of the hydrographic study at Wachapreague Inlet, the logistics of continuing the biological work increased steadily. Coupled with a greater need for biological information from other areas and the possibility of again cooperating with other personnel in this grant in collecting and developing this information, we decided in the winter of 1973 to terminate the biological work at Wachapreague. Since that time, our efforts have centered on the ecological aspects of the plankton community of the York River in anticipation of several imminent developmental projects in this area (i.e. channel dredging, sewage disposal plant, bilge water treatment plant, increased power plant capacity) with the potential to seriously alter this community.

Table 2.1

April 3, 1973 Stations X and Y
High Slack 0727 Low Slack 1340

| Time | Temp. (°C) | | Salinity (ppt) | | D.O. ($mgl^{-1}$) | | CHL."a" ($\mu gl^{-1}$) | | Vmax ($\mu gl^{-1}hr^{-1}$) | |
|---|---|---|---|---|---|---|---|---|---|---|
| | X | Y | X | Y | X | Y | X | Y | X | Y |
| 0740 | 8.8 | 8.9 | 30.23 | 30.13 | 8.08 | 7.94 | 4.26 | 3.66 | .46 | .87 |
| 0830 | 8.5 | 8.7 | 29.94 | 30.16 | 7.98 | 7.86 | 3.40 | 2.80 | .49 | .31 |
| 0930 | 8.7 | 8.8 | 30.19 | 30.21 | 8.22 | 8.38 | 3.90 | 3.36 | .29 | .42 |
| 1035 | 10.0 | 10.4 | 29.99 | 29.77 | | 8.28 | | 4.80 | .52 | .90 |
| 1135 | 11.1 | 11.2 | 29.70 | 29.68 | 8.34 | 8.44 | 4.50 | 4.64 | 1.07 | .88 |
| 1235 | 12.0 | 12.0 | 29.23 | 29.48 | 8.40 | 8.50 | | 3.90 | .95 | .70 |
| 1335 | 12.5 | 12.4 | 29.04 | 29.40 | 8.36 | 7.82 | 3.20 | 3.68 | .46 | .15 |
| 1440 | 12.5 | 11.8 | 28.72 | 29.49 | 8.24 | 8.32 | 3.20 | 1.76 | .41 | .55 |
| 1540 | 11.4 | 11.7 | 29.65 | 29.45 | 8.38 | 8.42 | 4.36 | 4.32 | .76 | .50 |
| 1642 | 8.5 | 10.6 | 30.29 | 29.84 | 8.14 | 8.22 | 5.24 | 4.20 | .74 | .61 |

Table 2.2

April 6, 1973 Stations X and Y
High Slack 0947 Low Slack 1551

| Time | Temp. (°C) | | Salinity (ppt) | | D.O. ($\mu gl^{-1}$) | | CHL"a" ($\mu gl^{-1}$) | |
|---|---|---|---|---|---|---|---|---|
| | X | Y | X | Y | X | Y | X | Y |
| 0940 | | 9.0 | | 30.18 | | 7.03 | | 3.8 |
| 1000 | 8.0 | 9.0 | 30.22 | 30.14 | 8.62 | 7.43 | 4.8 | 6.7 |
| 1020 | 9.5 | 9.2 | 30.19 | 29.88 | 7.96 | 6.75 | 3.9 | 4.1 |
| 1040 | 9.2 | 9.8 | 30.29 | 30.03 | 6.83 | 6.45 | 3.1 | 5.3 |
| 1100 | 9.5 | 9.3 | 30.20 | 30.06 | 7.90 | .84 | 4.1 | 4.1 |
| 1120 | 10.0 | 9.3 | 30.21 | 29.91 | 7.78 | 7.33 | 3.1 | 5.4 |
| 1140 | 10.0 | 9.6 | 30.21 | 29.87 | 8.50 | 7.56 | 3.7 | 6.0 |
| 1200 | | 9.8 | | 30.18 | | 5.99 | | 7.1 |
| 1220 | 10.5 | | 29.94 | | 8.14 | | 3.7 | |
| 1240 | 10.5 | | 29.92 | | 7.98 | | 4.0 | |
| 1300 | 11.0 | | 29.71 | | 6.93 | | 3.9 | |
| 1320 | 11.0 | 11.0 | 29.54 | 29.64 | 7.84 | 6.63 | 4.4 | 4.2 |
| 1340 | 11.5 | 11.2 | 29.45 | 29.12 | 7.96 | 6.83 | 3.1 | 5.3 |
| 1400 | 12.0 | 12.0 | 29.32 | 29.55 | 7.33 | 7.78 | 4.7 | 4.9 |
| 1420 | 11.8 | 11.9 | 29.30 | 29.57 | 7.03 | 6.81 | 3.7 | 5.6 |
| 1440 | 12.2 | 12.0 | 29.22 | 27.90 | 6.53 | 7.37 | 3.7 | 7.1 |
| 1500 | 12.2 | 12.1 | 29.15 | 29.54 | 7.19 | 7.80 | 3.5 | 6,1 |
| 1520 | 12.5 | 12.2 | 29.09 | 29.53 | 7.84 | 7.82 | 3.5 | 3.9 |
| 1540 | 13.0 | 12.4 | 28.95 | 29.52 | 7.78 | 8.04 | 3.6 | 5.1 |
| | | | | | Mean | | 3.7 | 5.3 |

Table 2.3

April 6, 1973
High Slack 0947

Offshore
Low Slack 1551

| Station | Time | Temp. ($^{o}C$) | Salinity (ppt) | D.O. ($mgl^{-1}$) | CHL"a" ($\mu gl^{-1}$) | Vmax ($\mu gl^{-1}hr^{-1}$) | Position |
|---|---|---|---|---|---|---|---|
| 1 | 0955 | 9.7 | 30.30 | 8.82 | 4.9 | .33 | - |
| 2 | 1011 | 10.0 | 30.30 | 8.64 | 3.7 | .20 | - |
| 3 | 1038 | 9.5 | 30.34 | 8.86 | 4.3 | .54 | - |
| 4 | 1055 | 10.0 | 30.17 | 8.94 | 4.0 | .36 | - |
| 5 | 1106 | 9.8 | 30.22 | 8.80 | 2.4 | .19 | out |
| 6 | 1117 | 10.0 | 30.13 | 8.78 | 3.8 | .24 | out |
| 7 | 1134 | 9.7 | 30.67 | 8.54 | 1.6 | .13 | out |
| 8 | 1153 | 10.5 | 29.42 | 8.60 | 0.8 | .17 | out |
| 9 | 1200 | 9.8 | 30.67 | 8.10 | 0.8 | .12 | out |
| 10 | 1220 | 9.7 | 30.69 | 8.44 | 1.6 | .21 | out |
| 11 | 1228 | 10.0 | 30.57 | 8.74 | 5.4 | .71 | - |
| 12 | 1240 | 10.5 | 30.37 | 8.16 | 3.7 | .35 | in |
| 13 | 1253 | 10.0 | 30.25 | 8.62 | 3.9 | .51 | in |
| 14 | 1308 | 10.7 | 30.09 | 8.40 | 5.1 | .68 | in |
| 3 | 1318 | 10.6 | 30.27 | 8.12 | 2.1 | .46 | - |
| 4 | 1323 | 10.0 | 30.03 | 8.20 | 2.1 | .43 | - |
| 5 | 1331 | 10.4 | 20.08 | 7.80 | 3.4 | .46 | in |
| 6 | 1339 | 10.5 | 30.02 | 8.02 | 3.5 | .34 | in |
| 7 | 1349 | 10.7 | 30.15 | 8.20 | 3.2 | .43 | in |

Table 2.3 (cont'd)

| Station | Time | Temp. ($^{o}C$) | Salinity (ppt) | D.O. ($mgl^{-1}$) | CHL"a" ($\mu gl^{-1}$) | Vmax ($\mu gl^{-1}hr^{-1}$) | Position |
|---|---|---|---|---|---|---|---|
| 8 | 1358 | 11.0 | 30.24 | 8.24 | 3.9 | .43 | - |
| 9 | 1406 | 10.8 | 29.94 | 7.70 | 3.8 | .50 | - |
| 10 | 1416 | 11.3 | 30.01 | 7.98 | 4.2 | .42 | - |
| 11 | 1427 | 10.0 | 30.43 | 8.22 | 4.4 | 1.21 | - |
| 12 | 1436 | 11.0 | 30.48 | 8.28 | 6.2 | .67 | in |
| 13 | 1445 | 11.2 | 29.80 | 8.26 | 5.8 | .71 | in |
| 14 | 1455 | 11.8 | 29.74 | 8.36 | 4.0 | .74 | in |
| 3 | 1506 | 12.0 | 29.79 | 8.44 | 3.6 | .63 | - |
| 13 | 1520 | 11.7 | 29.80 | 8.32 | 3.4 | .51 | in |
| 2 | 1535 | 12.5 | 29.48 | 8.20 | 3.8 | .48 | in |
| 1 | 1544 | 12.5 | 29.30 | 8.10 | 3.0 | .51 | in |
| in plume (n=12) | | 11.21 | 29.97 | 8.22 | 4.14 | .53 | |
| out plume (n=6) | | 9.91 | 30.30 | 8.54 | 1.86 | .17 | |

Table 2.4

May 30-31, 1973 — Stations A,D,X and Y
High Slack 0551; 1812 — Low Slack 1148

| Time | Temp. ($^{o}C$) | | Salinity (ppt) | | D.O. ($mgl^{-1}$) | | K ($m^{-1}$) | | CHL"a" ($\mu gl^{-1}$) | | Vmax ($\mu gl^{-1}hr^{-1}$) | |
|---|---|---|---|---|---|---|---|---|---|---|---|---|
| | X | Y | X | Y | X | Y | X | Y | X | Y | X | Y |
| 0815 | 17.8 | 17.8 | 31.53 | 31.56 | 7.46 | 7.26 | 1.66 | 1.72 | 3.44 | 4.12 | .62* | .50* |
| 0910 | 18.0 | 18.2 | 31.51 | 31.54 | 7.68 | 7.50 | 2.00 | 2.22 | 2.20 | 3.40 | .63* | .56* |
| 1003 | 19.8 | 19.5 | 31.44 | 31.46 | 7.38 | 7.28 | 1.54 | 1.88 | 2.80 | 2.6[illegible] | .90* | .92* |
| 1103 | 20.2 | 20.4 | 31.42 | 31.47 | 7.42 | - | 3.12 | 1.54 | 2.32 | 1.92 | .99* | .94* |
| 1215 | 21.4 | 21.4 | 31.30 | 31.49 | 7.16 | 7.24 | 1.54 | 2.04 | 3.00 | 2.44 | 1.11* | 1.04* |
| 1310 | 21.4 | 21.4 | 31.35 | 31.51 | 7.40 | 7.14 | 1.49 | 1.54 | - | - | .78* | .66* |
| 1412 | 21.0 | 21.0 | 31.31 | 31.48 | 7.38 | 7.16 | 1.82 | 1.54 | 1.96 | 2.08 | .55 | .55 |
| 1519 | 20.5 | 20.2 | 31.47 | 31.48 | 7.56 | 7.38 | 2.04 | 3.57 | 4.36 | 3.44 | .84 | .43 |
| 1603 | 18.6 | 18.2 | 31.56 | 31.56 | 7.26 | 7.48 | 2.38 | 2.50 | 4.96 | 5.28 | .72 | .[illegible] |
| 1703 | 18.0 | - | 31.56 | 31.57 | 7.76 | 7.94 | 2.22 | 2.5[illegible] | 5.64 | 5.10 | .68 | .59 |
| 1803 | 18.0 | 18.0 | 31.58 | 31.58 | 7.40 | 7.72 | 2.32 | 2.50 | 4.70 | 3.92 | .63 | .58 |
| 1847 | 17.6 | 17.9 | 31.58 | 31.58 | 7.76 | 7.86 | 2.50 | 2.00 | 3.76 | 5.52 | .45 | .02 |
| | A | | A | | A | | A | | A | | A | |
| 0700 | 22.0 | | 30.08 | | 6.40 | | - | | 1.76 | | 1.18 | |
| 1345 | 35.2 | | 33.14 | | - | | - | | 22.16 | | 32.20 | |
| 1945 | 19.8 | | 31.54 | | 7.50 | | - | | 4.28 | | .47 | |
| | D | | D | | D | | D | | D | | D | |
| 0750 | 18.5 | | 31.53 | | 7.46 | | 1.26 | | 2.04 | | - | |
| 1245 | 19.0 | | 31.49 | | 7.54 | | 1.66 | | 1.88 | | .21 | |
| 1825 | 19.0 | | 31.58 | | 7.60 | | 1.26 | | 2.84 | | .04 | |
| | IN | OUT | IN | OUT | IN | OUT | IN | OUT | IN | OUT | IN | OUT |
| 1320 | 19.5* | 18.8* | 31.62* | 31.58* | 6.62* | 6.48* | 1.45* | .69* | - | - | .73* | .13* |

* These values from samples taken on 31 May.

Table 2.5

July 2, 1973 Stations 1',2',3',4',
High Slack (HS) 1006 Low Slack (LS) 1612

Temp
($^{o}C$)

| | 1' | 2' | 3' | 4' | | |
|---|---|---|---|---|---|---|
| HS | 20.8 | 22.0 | 22.4 | - | In* | 22.24 |
| ME | 21.9 | 21.0 | 22.1 | 22.2 | | |
| LS | 24.0 | 23.5 | - | 23.0 | Out* | 22.34 |

D.O.
($mgl^{-1}$)

| | 1' | 2' | 3' | 4' | | |
|---|---|---|---|---|---|---|
| MS | - | - | - | - | In | 6.20 |
| ME | 6.32 | 6.14 | 6.78 | 6.84 | | |
| LS | 6.16 | 6.24 | 6.14 | 6.96 | Out | 6.80 |

K
($m^{-1}$)

| | 1' | 2' | 3' | 4' | | |
|---|---|---|---|---|---|---|
| HS | 1.75 | - | .91 | .88 | In | 1.86 |
| ME | 2.12 | 2.00 | 1.00 | 1.05 | | |
| LS | 1.43 | 2.00 | 1.66 | 1.08 | Out | .98 |

CHL"a"
($\mu gl^{-1}$)

| | 1' | 2' | 3' | 4' | | |
|---|---|---|---|---|---|---|
| HS | 8.95 | 8.32 | 7.00 | 5.44 | In | 6.61 |
| ME | 6.45 | 7.50 | 7.65 | 8.32 | | |
| LS | 4.15 | 6.60 | 6.10 | 6.45 | Out | 7.19 |

Primary Production
($mgCm^{-3}hr^{-1}$)

| | 1' | 2' | 3' | 4' | | |
|---|---|---|---|---|---|---|
| HS | 17.14 | 12.47 | 11.66 | 6.85 | In | 14.88 |
| ME | 19.00 | 13.30 | 13.00 | 17.23 | | |
| LS | 16.94 | 12.93 | 10.00 | 5.90 | Out | 12.85 |

Vmax
($\mu gl^{-1}hr^{-1}$)

| | 1' | 2' | 3' | 4' | | |
|---|---|---|---|---|---|---|
| HS | 2.22 | .20 | .19 | .08 | In | .95 |
| ME | .84 | .75 | .31 | .19 | | |
| LS | .49 | .88 | .55 | .20 | Out | .20 |

* These values are averages of stations in and out of the plume. Stations 1'HS, 1'ME, 1'LS, 2'HS, 2'ME and 3'LS were in the plume. Stations 2'HS, 3'HS, 3'ME, 4'HS, 4'ME and 4'LS were out of the plume.

Table 2.6

July 3, 1973
Low Slack 0353

Stations A, B, X and Y
High Slack 0959

| Time | Temp (°C) | | D.O. ($mgl^{-1}$) | | K ($m^{-1}$) | | Chl "a" ($\mu gl^{-1}$) | | Primary Prod. ($mgm^{-3}hr^{-1}$) | | Vmax ($\mu gl^{-1}hr^{-1}$) | |
|---|---|---|---|---|---|---|---|---|---|---|---|---|
| | X | Y | X | Y | X | Y | X | Y | X | Y | X | Y |
| 0604 | 24.0 | 24.0 | 5.78 | 5.86 | - | - | 4.40 | 3.76 | 11.52 | 15.73 | - | .86 |
| 0717 | 23.1 | 23.6 | 6.34 | 5.84 | 2.63 | 2.50 | 5.04 | 4.72 | 7.54 | 5.49 | .91 | .81 |
| 0825 | 22.0 | 21.9 | 6.20 | 6.08 | 1.69 | 2.04 | 5.64 | 5.80 | 19.17 | 15.84 | .81 | .75 |
| 0923 | 21.5 | 21.6 | - | 6.42 | 1.69 | 2.00 | 7.48 | 6.32 | 17.24 | 12.03 | .68 | .77 |
| 1013 | 21.8 | 21.6 | 6.52 | 5.98 | 1.47 | 1.54 | 7.08 | 6.04 | 16.94 | 14.20 | - | .43 |
| 1145 | 21.8 | 21.8 | 6.36 | 6.14 | 1.54 | 2.08 | 7.40 | 9.04 | 10.41 | 13.31 | .48 | .47 |
| 1307 | 22.0 | 21.5 | 6.00 | 6.22 | 1.37 | 1.43 | 24.3 | 5.44 | 8.51 | 11.02 | 1.02 | 1.15 |
| 1404 | 23.8 | 22.8 | 6.44 | 6.16 | 1.82 | 1.82 | 7.20 | 5.40 | 11.0 | 11.83 | .94 | .85 |
| 1521 | 24.8 | 24.5 | 6.34 | 5.80 | 2.27 | 2.22 | 5.08 | 5.64 | 17.68 | 8.46 | 1.94 | .76 |
| 1615 | 25.3 | 25.4 | 5.90 | 5.76 | 1.66 | 2.04 | 6.24 | 6.48 | 15.49 | 13.06 | 1.53 | 1.05 |
| 1708 | 26.0 | 26.0 | 5.58 | 5.80 | 2.00 | 1.54 | 7.08 | 7.76 | 12.20 | 13.63 | 1.25 | 1.14 |
| | A | B | A | B | A | B | A | B | A | B | A | B |
| 0600 | - | - | - | - | - | - | 13.60 | 7.60 | 49.70 | 18.61 | 12.65 | 2.52 |
| 1100 | 24.5 | 24.[illegible] | 5.76 | 5.58 | - | - | 4.00 | 5.46 | 11.37 | 11.78 | 1.75 | 1.06 |

Table 2.7

September 25, 1973 Station Y
High Slack 0630, 1846 Low Slack 1240

| Time | Temp (°C) | Sal (ppt) | D.O. ($mgl^{-1}$) | K ($m^{-1}$) | Chl "a" ($\mu gl^{-1}$) | Primary Prod. ($mgm^{-3}hr^{-1}$) | Vmax ($\mu gl^{-1}hr^{-1}$) |
|---|---|---|---|---|---|---|---|
| 0800 | 22.5 | 31.13 | 7.00 | 2.7 | 5.3 | 7.85 | .62 |
| 0900 | 22.5 | 31.07 | 6.80 | 2.7 | 5.3 | 7.43 | .40 |
| 0945 | - | 31.68 | 7.12 | 2.9 | 5.8 | 9.05 | .45 |
| 1030 | 22.5 | 31.08 | 7.20 | 3.7 | 5.9 | 8.51 | .98 |
| 1115 | 22.5 | 31.14 | 7.00 | 4.3 | 5.1 | 9.96 | .53 |
| 1220 | 22.8 | 31.18 | 6.70 | 4.2 | 7.3 | 13.37 | .80 |
| 1250 | 22.8 | 31.20 | 6.80 | 5.0 | 8.3 | 12.07 | .76 |
| 1330 | 22.9 | 31.20 | 6.60 | 4.0 | 7.6 | 12.9 | .76 |
| 1415 | 22.9 | 31.26 | 6.72 | 3.3 | 6.6 | 12.69 | .48 |
| 1500 | - | 31.23 | 6.84 | 2.9 | 7.6 | 10.34 | .65 |
| 1545 | 22.9 | 31.21 | 6.92 | 5.0 | 10.1 | 11.91 | .45 |
| 1630 | 23.0 | 31.14 | 7.02 | 4.5 | 9.12 | 12.82 | .57 |
| 1715 | 22.6 | 31.09 | 7.42 | 5.3 | 8.30 | 13.52 | .84 |
| 1815 | 22.5 | 31.05 | 7.40 | 5.0 | 8.32 | 9.95 | .96 |

Table 2.8

November 11, 1973
High Slack 0742 Low Slack 1421

| Station | Time | Temp (°C) | Sal (ppt) | K ($m^{-1}$) | Chl "a" ($\mu g l^{-1}$) | Vmax ($\mu g l^{-1} hr^{-1}$) |
|---|---|---|---|---|---|---|
| 1 | 1030 | 13.15 | 31.59 | .80 | 3.65 | .072 |
| 2 | 1200 | 13.12 | 31.56 | .71 | 3.65 | .072 |
| 3 | 1310 | 13.25 | 31.54 | .86 | 2.97 | .087 |
| 4 | 1420 | 9.58 | 30.89 | 1.66 | 2.74 | .160 |
| 5 | 1525 | 10.61 | 31.01 | 1.15 | 2.40 | .155 |
| 6 | 1620 | 12.90 | 31.39 | .79 | 2.17 | .065 |

Table 2.9

November 12, 1973
High Slack 0831 Low Slack 1510

| Station | Time | Temp (°C) | Sal (ppt) | K ($m^{-1}$) | Chl "a" ($\mu g l^{-1}$) | Vmax ($\mu g l^{-1} hr^{-1}$) |
|---|---|---|---|---|---|---|
| 7 | 0735 | 11.68 | 31.12 | 1.05 | 15.83 | .089 |
| 8 | 0907 | 11.82 | 31.13 | .85 | 6.43 | .118 |
| 9 | 1018 | 12.84 | 31.43 | .80 | 6.44 | .045 |
| 10 | 1055 | 12.99 | 31.53 | .70 | 2.40 | .100 |
| 11 | 1130 | 11.37 | 31.21 | 1.29 | 5.40 | .231 |
| 12 | 1210 | 12.14 | 31.12 | .81 | 5.39 | .064 |
| 13 | 1255 | 11.05 | 31.02 | 1.00 | 7.65 | .134 |
| 14 | 1335 | 12.28 | 31.25 | .82 | 8.00 | .067 |
| 15 | 1412 | 11.06 | 31.04 | .84 | 7.83 | .121 |
| 16 | 1500 | 11.93 | 31.00 | .71 | 7.13 | .213 |

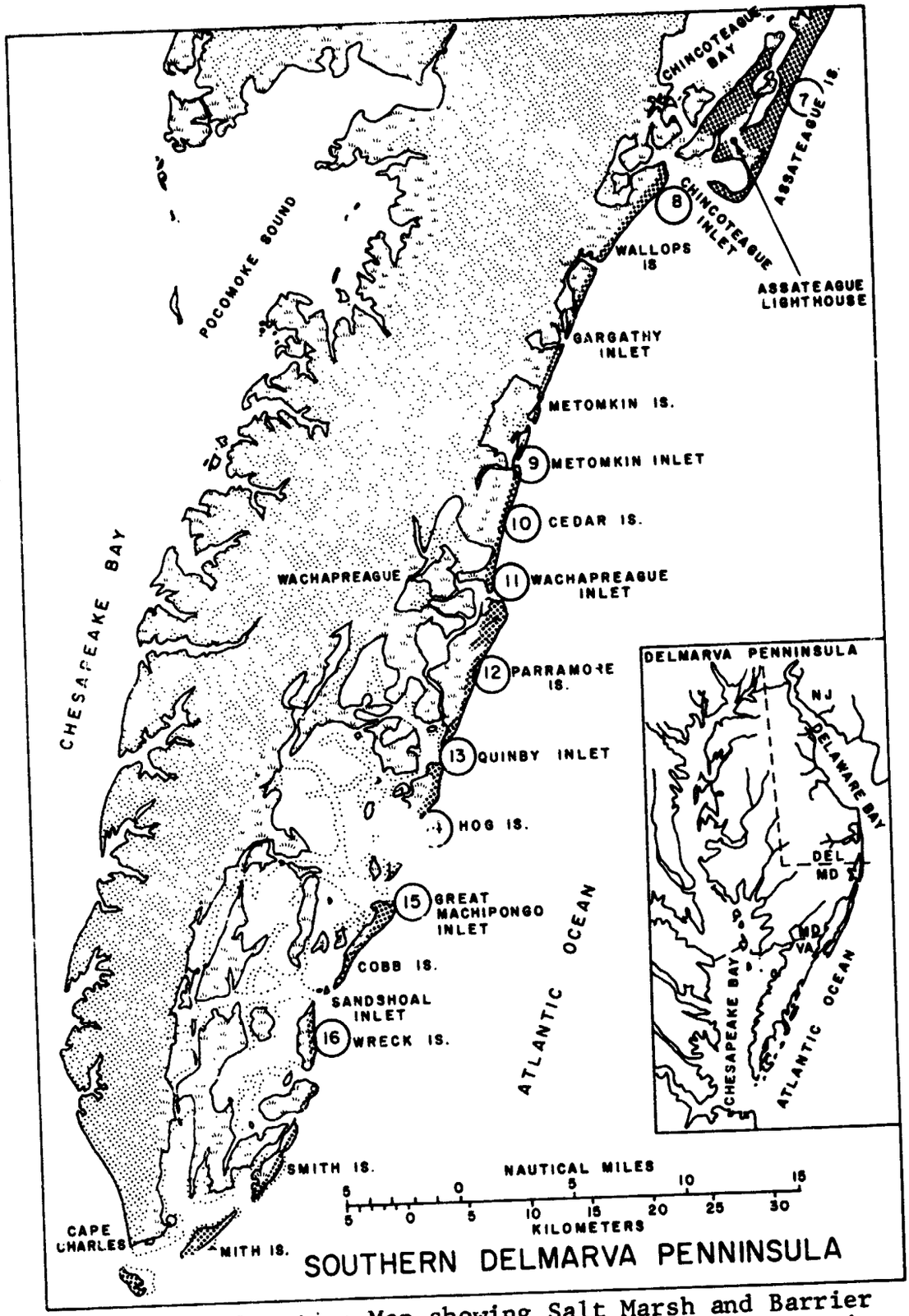


Figure 2.1. Location Map showing Salt Marsh and Barrier Islands of Eastern Shore, Virginia. Stations 7-16 Sampled on November 12, 1973.

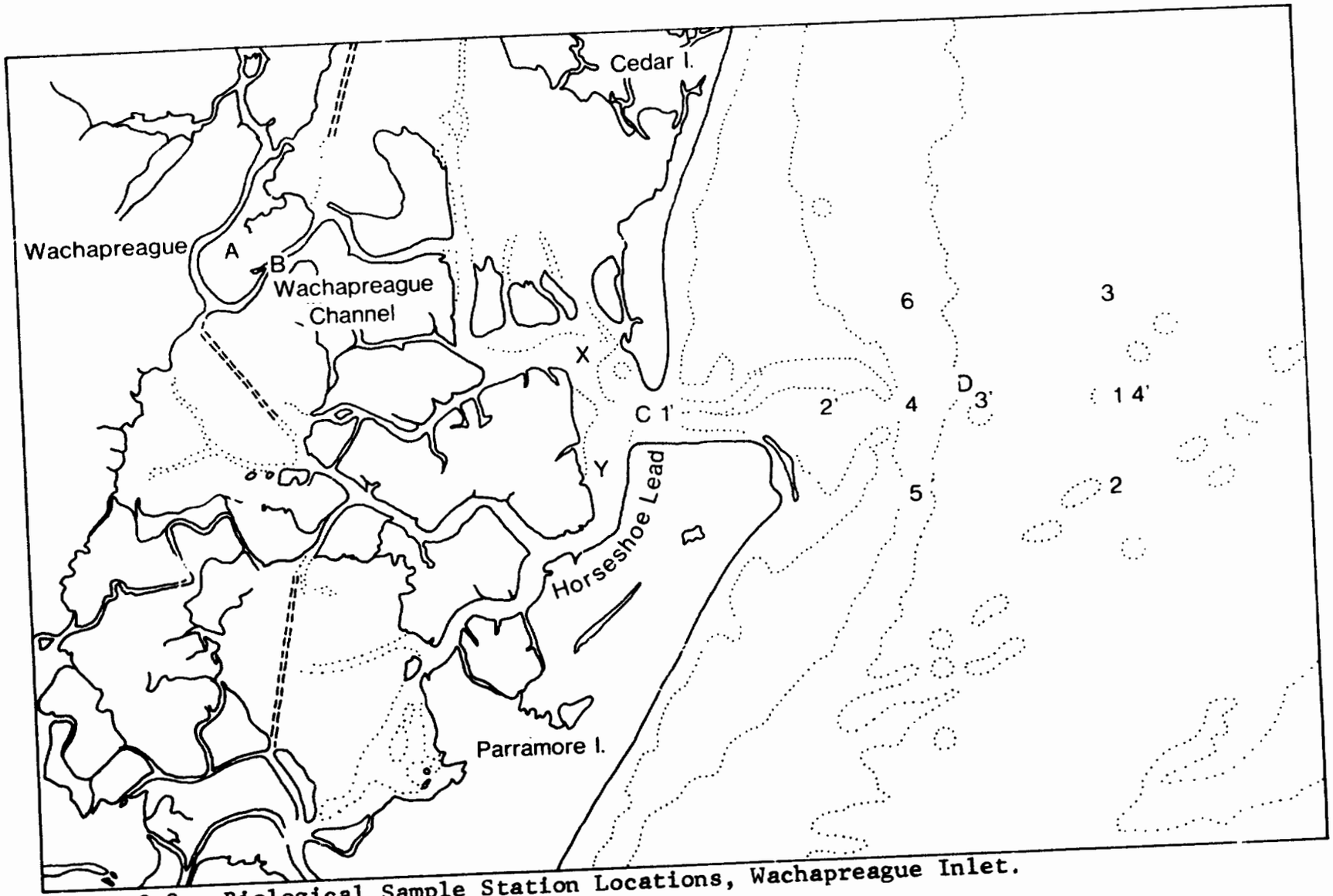


Figure 2.2. Biological Sample Station Locations, Wachapreague Inlet.

## APPENDIX 3

## DEVELOPMENT OF A REMOTE NAVIGATION SYSTEM FOR TRACKING FREE DRIFTING BUOYS

### Introduction

The requirement for a capability to accurately track drifting buoys has been long standing within the oceanographic world. Many types of systems have been developed and no attempt will be made here to describe them. Suffice to say that most have met with limited success for one reason or another.

Within the confines of this grant, it is felt that a means of ground truthing water circulations is necessary to substantiate the findings noted in the various remote sensing techniques.

With this requirement in mind, the development of a buoy tracking system has been undertaken. We have based our work on that of Dr. E. Michelena who in fact developed a pilot system utilizing the Omega Navigation Network for determining buoy positions. His work showed that indeed such a system was feasible, the next logical step being to build and deploy an actual prototype.

### Brief Description of the Omega System

Omega was developed by the Navy in order to provide worldwide positioning information to its ships. The network is serviced by a total of eight stations throughout the world:

Norway, Trinidad, Hawaii, North Dakota, Reunion, Argentina, Japan and Australia. The first four will all be operational in August of this year (1974); the others are in planning stages. They all broadcast at a frequency of 10.2 kHz in the format shown schematically in Figure 3.1.

Worldwide coverage is achieved due to the extremely long propagation of radio waves at 10.2 kHz. Stations are identified by noting the pattern of transmissions. One of the advantages of the system is that the electronics to derive the necessary position information is relatively simple.

Each pair of stations has a family of curves of equal phase difference called lines of position (LOP's) associated with it. Two LOP's (three stations) are required for a fix.

The advertised accuracy of fixes in the Omega System is three nautical miles (5.5 km). This fairly large error is due to the many unknown factors affecting the transmission paths of the signals. These are due to regular diurnal shifts of the ionsphere and random atmospheric noise due, for instance, to thunderstorms and sunspots. The diurnal shift is fairly predictable and correction tables have been published that account for much of this error source. The others are entirely unpredictable and in severe cases can cause total data drop out. Often a good track determination becomes a game of statistics.

A mode of operation of the system termed "differential" eliminates much of the local error due to some of these sources. In this mode the LOP's of a fixed location are determined from signal receptions and from actual LOP's plotted

on a chart. The two are compared and a differential error calculated which can be applied to other data taken in the same locale. A reasonable assumption is made here that the errors within a 50 km range are approximately the same at the same point in time. It is hoped that an accuracy of 0.15-1 km can be obtained by utilizing this scheme in our system.

Areas where good reception has been noted include the Eastern Shore of Virginia, Hampton, Virginia, NASA/Langley Research Center and Hampton Roads. Reception has been good enough to justify the utilization of Omega in our system.

VIMS itself has proved to be a poor location for Omega reception due to much power line noise and the Coleman Bridge which shorts much of the signal to ground. This problem is felt to be local and moving a few hundred yards up or down river is expected to improve matters.

The Scheme of our Development

Our approach is to build a cheap, simple buoy and electronics package that will receive the Omega signals and retransmit them via a 2.398 MHz telemetry link to a base station. There they will be reconstructed and input to a commercial Omega processor for determination of buoy LOP's. To achieve "differential Omega" the base station LOP's will also be determined. All of this information is input to a Data General 1220 mini computer for storage, correction, and averaging.

Brief Description of the Buoy System

The buoy electronics consist of three basic subsystems as noted in Figure 3.2. Every effort is being made to keep the weight and cost of these as small as possible in order to make them "throw away" items. This is done in view of the expense of ship time to retrieve them should they drift long distances. A brief description of each subsystem follows.

The Omega signal at 10.2 kHz is to be received by an antenna hanging down from the buoy in the water. This configuration is desirable in order to eliminate radio frequency interference, particularly that of the telemetry link, from the input signal. (RF frequencies are greatly attenuated by seawater.) The signal is then fed into a highly sensitive narrow band-width receiver and amplified. After amplification the 10.2 kHz signal is fed to the transmitter to modulate a 2.398 MHz telemetry link. An experimental FCC license has been obtained to transmit in the single side band mode with only the low side band suppressed, the carrier and high side band being transmitted. Power for the system is provided by two lead-acid automobile batteries and supplied through a switching circuit triggered by a crystal controlled clock. Should power requirements indicate, it would be desirable to use smaller batteries. The accuracy of the clock is within a few seconds per day. In the initial system of five buoys the clocks will be set to turn on each buoy sequentially for a ten minute period. Thus, each buoy will be identified by the time slot during which it is active.

Brief Description of the Base Station

The base station consists of the three subsystems noted in Figure 3.3. They will eventually be assembled in a mobile van or hut for on site operation.

The receiver demodulator is unique in that it is required to have a 10.2 kHz bandwidth, and the demodulation technique must carefully preserve the phase relationships of the original Omega signals. These are not normally requirements in commercial receivers. It has been necessary to contract out the job of constructing this receiver to the Biological Instrumentation Systems firm in Newport News.

The LITCOM ORN-101 Omega receiver is the heart of base station and indeed the entire system. It receives and processes signals sequentially from each buoy and in its own time slot, a signal from its own antenna.

The processor in the ORN-101 consists of a small dedicated mini computer that synchronizes on the input signals and determines the phase relationships between them. Two lines of position (LOP's) are chosen on its front panel via thumb wheel switches and these are displayed via a Nixie tube readout. Also displayed is a signal quality indication that shows when the signal to noise ratio of an incoming signal is greater than 1:10.

The ORN-101 must be switched between several signals, that from its own antenna and those from the buoys. At each switching the phase locks must be re-attained. This process, which may take several minutes, places a lower limit on sampling intervals.

As large amounts of data will need to be processed, averaged, corrected and stored, the ORN-101 was purchased with an interface to a Data General 1220 mini computer. The two LOP's, time and signal quality information, are output in a binary format to the 1220.

The Data General system consists of central processor, 1/2 inch tape drive unit, teletypewriter and cassette tape drive unit. Programs are being developed to handle the incoming data.

System Status

Buoy

The buoy electronics are being designed and constructed by VIMS and are at the following stages of completion:

| | |
|---|---|
| Power transmitter | 85% |
| Modulator | 90% |
| Oscillator | 100% |
| Receiver | 80% |
| Crystal Clock | 80% |
| Power Switching Circuit | 0% |

It is expected that the entire buoy electronics system will be packaged and integrated by 1 November.

No hardware for the buoy itself has been finally designed. The shape and size will depend on what the electronics and power supply look like. Our initial test bed will be a boat-shaped surplus rocket launcher. This can be moored and is convenient to work from.

Base Station

The base station receiver is being constructed by Biological Instrumentation Systems. We have asked them for a delivery date of 30 September.

The LITCOM ORN-101 Omega receiver has not been fully tested. This has been due to two factors: The Omega network has not been up for much of the last year so no signals were available for testing. When they were available they were of poor quality due to poor reception at VIMS.

The other facet of the ORN-101 requiring checkout is the mini computer interface. The interface has been built and the hardware is currently operating, with signals having been transferred successfully to the NOVA 1220.

The Data General 1220 mini computer system is installed and functioning. Several programmers have been utilizing it, familiarizing themselves with the various capabilities and quirks of the system. A program has been written to exercise the interface to the LITCOM ORN-101.

We expect to begin full scale field testing on 1 November of this year (1974).

# OMEGA

WORLD WIDE NAVIGATION SYSTEM OF 8 STATIONS. WE WILL USE FOUR STATIONS.

A. NORWAY
B. TRINIDAD
C. HAWAII
D. NORTH DAKOTA

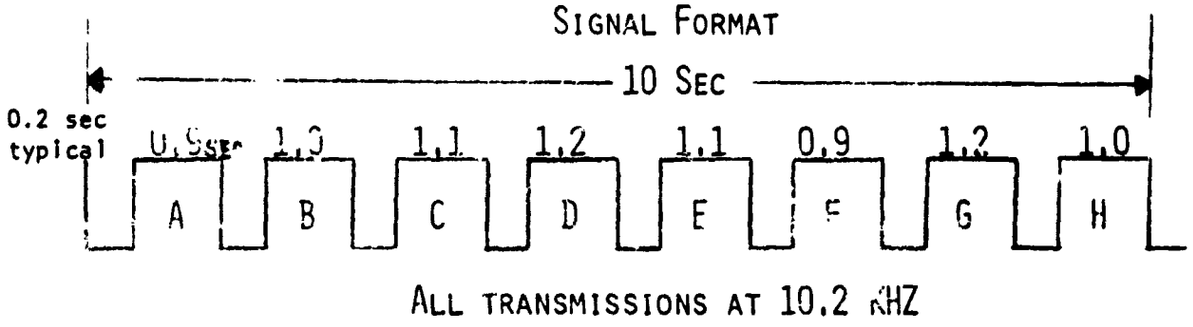


ALL TRANSMISSIONS AT 10.2 KHZ

LINES OF POSITION LOP'S ARE DEVELOPED FROM PHASE DIFFERENCES BETWEEN STATIONS.

BASIC SYSTEM ACCURACY OF 1 - 5.5 KM.

DIFFERENTIAL MODE ACCURACY OF 0.15 - 1 KM.

LARGE VARIATIONS IN SIGNAL RECEPTION DUE TO DIURNAL SHIFTS OF IONOSPHERE AND OTHER ATMOSPHERIC NOISE.

Figure 3.1. Omega Format.

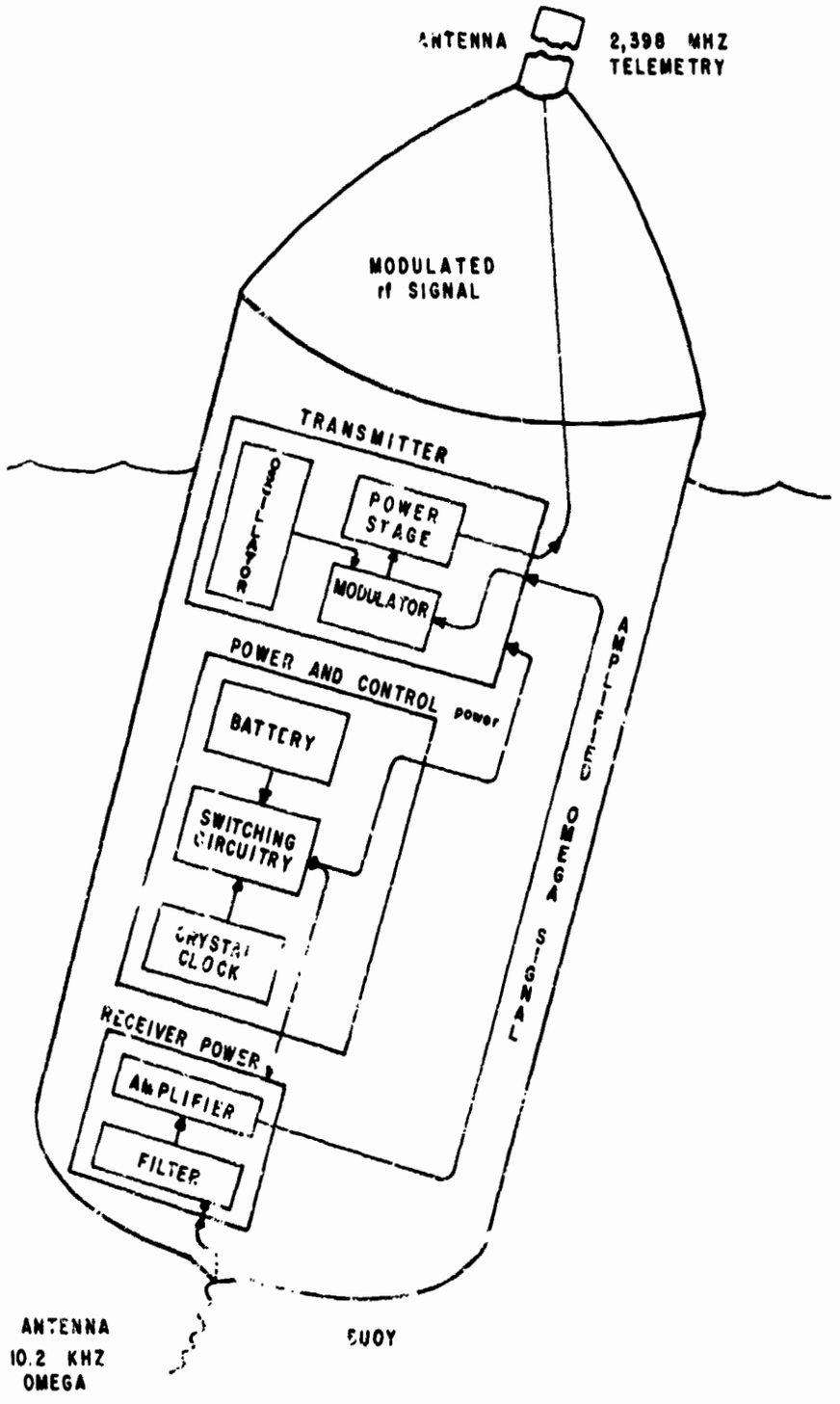


Figure 3.2. Buoy System.

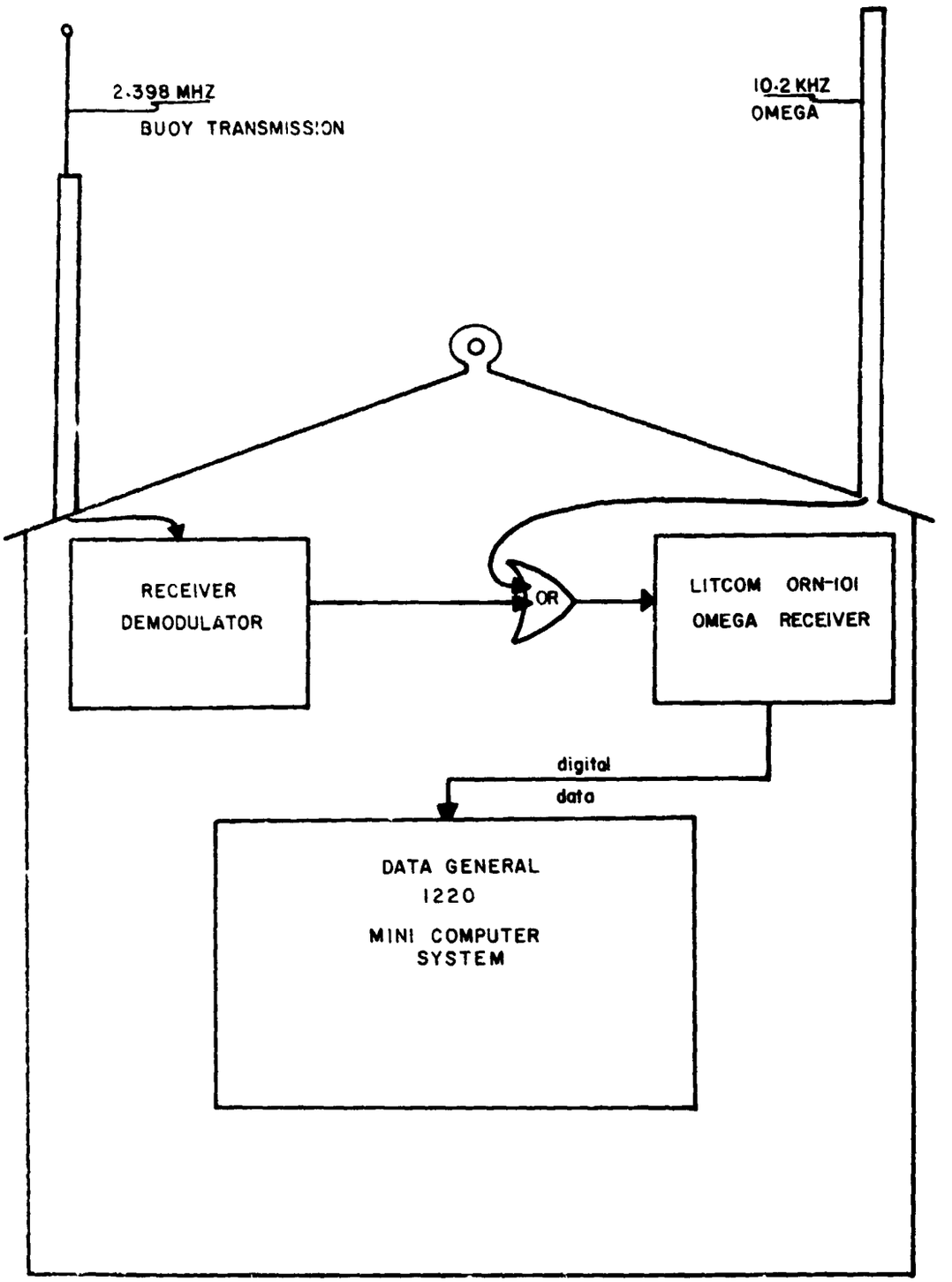


Figure 3.3. Mobile Base Station.

## APPENDIX 4

### EXPERIMENTAL DESIGN OF AN ESTUARINE TIDAL CIRCULATION STUDY EMPLOYING REMOTE SENSING

Remote sensing techniques have made possible a significant advance in estuarine tidal flow determinations. The following is a description of a study we plan to undertake next year which takes nearly full advantage of such advances.

The determination of surface water currents from aerial photographs has been reported on extensively. The techniques have involved interpretation of sequential images using various identifiable "targets" on the water surface. These have been either converted to equivalent topography through standard photogrammetric methods or located directly with respect to fixed points on the two photographs. Either technique is ideally suited for work in the Virginia estuaries, because image position can easily be related to landmarks using images obtained from moderate heights. An extension to continental shelf work may be possible by using a technique referred to in Yeske, et al (1973).

A weakness in image analysis for determination of current velocities is its dependence on targets. The velocity of the water is inferred by determining the velocity of something visible in the water. Such objects can be affected by both wind and wave induced drag, if they are large enough to be detected in the image. Natural targets, in particular foam slicks occur because of singularities in the flow field,

notably regions of great convergence and shear flow. They are valuable in images for that reason, but can be expected not to reflect a typical velocity of the water.

The weakness is inherent in the method, but can be greatly reduced by appropriate target design. The target we have designed consists of a small float($\sim$ 135 $cm^2$ projected area) attached to a window shade drogue (Monahan, et al, 1973) with a 1 square meter cross section area. This results in a frontal area ratio of 73 to 1 and a resulting velocity error of 12% of the velocity difference between the surface float and the drogue (Welch & Haas, 1973). The float has about 2 cm free-board and contains a cast slug of 10% polyvinyl alcohol 90% uranine dye mixture. This mixture releases dye for several hours producing a dye patch visible from a 5000 ft elevation aerial photograph. The patches should last for a six hour half tidal cycle.

The use of remote sensing and image analysis has resulted in two significant improvements in the technique. The first is that the effort of direct wind on the drogued buoy assembly is virtually eliminated. This not only reduces the sources of error, but it reduces them to a point where the first order correction to the primary source of error can be calculated from data available in the images. In addition, the appearance of the dye plume gives an independent qualitative estimate of the importance of the remaining primary error source. The second improvement is that the number of independently tracked targets which can be followed during a given experiment

increases at least twentyfold over previously used techniques. This increase will allow us to obtain for the first time a synoptic survey of a half tidal cycle of current in an estuary.

The survey will introduce us to a large scale data handling problem which has been alluded to by several previous investigators. Groen, et al (1971) chose 21 of 172 photographs in which a total of 81 x 3 or 243 separate points are located in an estimate of oceanic diffusion. They are able, for the most part, to identify individual targets from one photograph to the next by pattern recognition of the tarbet "swarm". With a similar problem, Djuric and Leribaux (1974) break up a cluster of floating objects into subgroups on a predetermined grid and make no attempt to identify individuals between successive photographs. Whe- a large number of points is used, the implicit pattern recognition technique of photogrammetric current measurement (Cameron, 1952; Yeske, et al, 1973, for example) is used to obtain each of two components of current velocity in turn.

In the proposed study, a somewhat new method will be used to solve the problems of target identification and velocity field determination. The first step in data processing for a given frame will be to locate by horizontal coordinates as many of the dye targets as are visible. These will then be placed in a horizontal coordinate grid on the earth using identifiable landmarks in the photographs and the predetermined coordinates of the landmarks. Individual identification of the points will be done by association of the observed points with

a prediction based on previous data. The correspondence which produces the least square error in the total predicted minus observed position field between photographic runs will be chosen as the identification field for the new set of positions. The square root of the error field divided by the total travel distance between successive images can be used as a figure of meri from which estimates of greatest allowable time between photographic runs can be produced.

The entire data reduction procedure is adaptable to machine processing from the initial scanning of photographs to the final production of a smoothed velocity field. The manual inclusion of apparent velocity discontinuities can also be added to the data processing. Finally, several qualitative indicators can be obtained from the appearance of the dye streaks. The signatures of surface and subsurface drogued buoy fields are likely to differ, and a buoy fields are likely to differ, and a buoy aground is going to produce a much different dye streak than one afloat. In the future, a buoy may be designed which seals off the dye ports if the tension on the drogue is severely reduced, a sign that the drogue has become separated from the buoy.

The identification of buoys on successive runs depends to some degree on the predicted velocity field. Such a field must be built up for the first few sets of images in a given experiment. The initial construction of this field must be done from the first two sets of photographs using direct pattern recognition. For this reason, the first two sets of

photographs must be more closely spaced in time than later ones. In addition, a regular grid of well spaced initial positions for buoy deployment will be very helpful in producing the initial identification field.

As a moderately large number of objects will be strewn in the estuaries of Virginia during this study, some thought has been directed to the materials from which the targets are constructed. In particular, materials have been sought which will, in the course of a year or so, be converted into biologically assimilable substances with the thought that a small increase in biological and chemical oxygen demand is preferable to the creation of indestructable litter. The resulting construction of the targets is from unpainted wood and muslin. The attachment cord is still a synthetic fiber, as the breaking strength of cotton string is much less for a given cross section. As we gain experience handling the targets in the field, we may be able to substitute an assimilable fiber string in the design.

The experiments resulting from this design work should prove to be easy to run, highly informative, compatible with modern data analysis techniques without sacrificing the qualitative advantages of photographic analysis, and non-exacerbating to those problems to which they are addressed.

## APPENDIX 5

## SKYLAB SUPPORT WORK

The SKYLAB support mission was run on May 31, 1973, using the technique which had been developed the previous year in the James River and at Wachapreague Inlet. Our effort was again supported by personnel and a radar from NASA/Wallops Island Station as well as personnel and equipment from NASA/Langley Research Center. The principal investigator at VIMS was Dr. Maynard Nichols of the Department of Geological Oceanography. The raw data were supplied to Dr. Nichols.

The positions of deployment of the buoys as well as their subsequent tracks are shown in Figure 5.1. The corresponding velocities calculated have their speeds displayed in Figure 5.2. They fall within the range of speeds predicted near the area the buoys drifted through in the tide tables, which are shown with a vertical bar on the same chart.

Several features of the ebb flow through the Chesapeake Bay mouth are apparent in these displays, the first being a convergence of surface water towards Cape Henry on ebb tide. This is consistent with other observations of the flow through the Bay mouth, although the extent of the convergence is somewhat surprising. The second feature apparent is that the speeds offshore are greater than those in the Bay. Less evident is the fact that the offshore track followed an extension of the Chesapeake Channel and went outside of the

first offshore bar. The increase in speed may be due to a phase shift in the tidal wave between Chesapeake Bay and the Atlantic Ocean or due to a relaxing of the bottom friction effect in deeper water such as was observed in the James River Drogue Study (Welch & Haas, 1973). In any case, the sudden and dramatic acceleration observed in the Wachapreague Inlet case was not reproduced at the mouth of Chesapeake Bay.

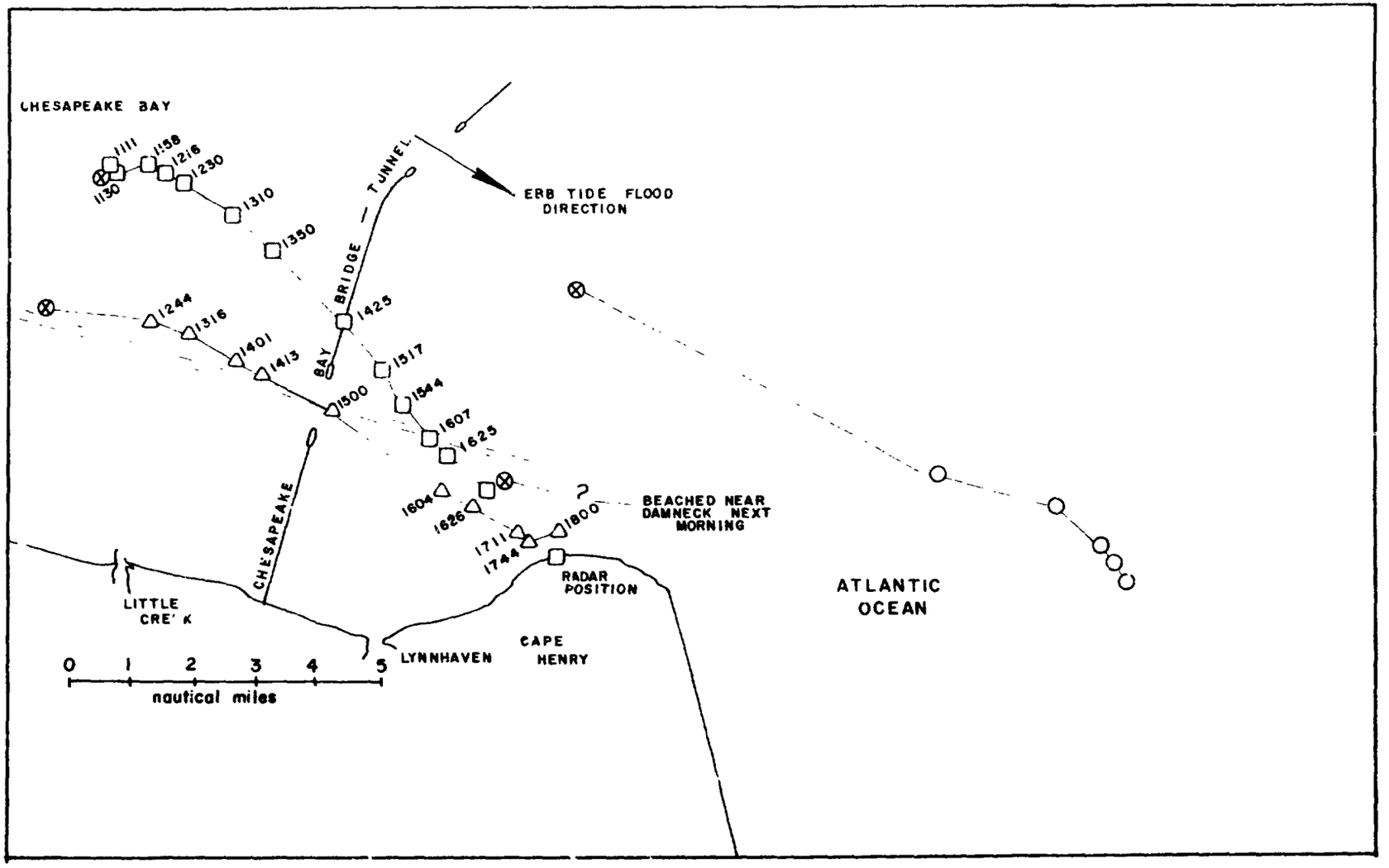


Figure 5.1. Buoy Positions, SKYLAB Support Project, 31 May 1973.

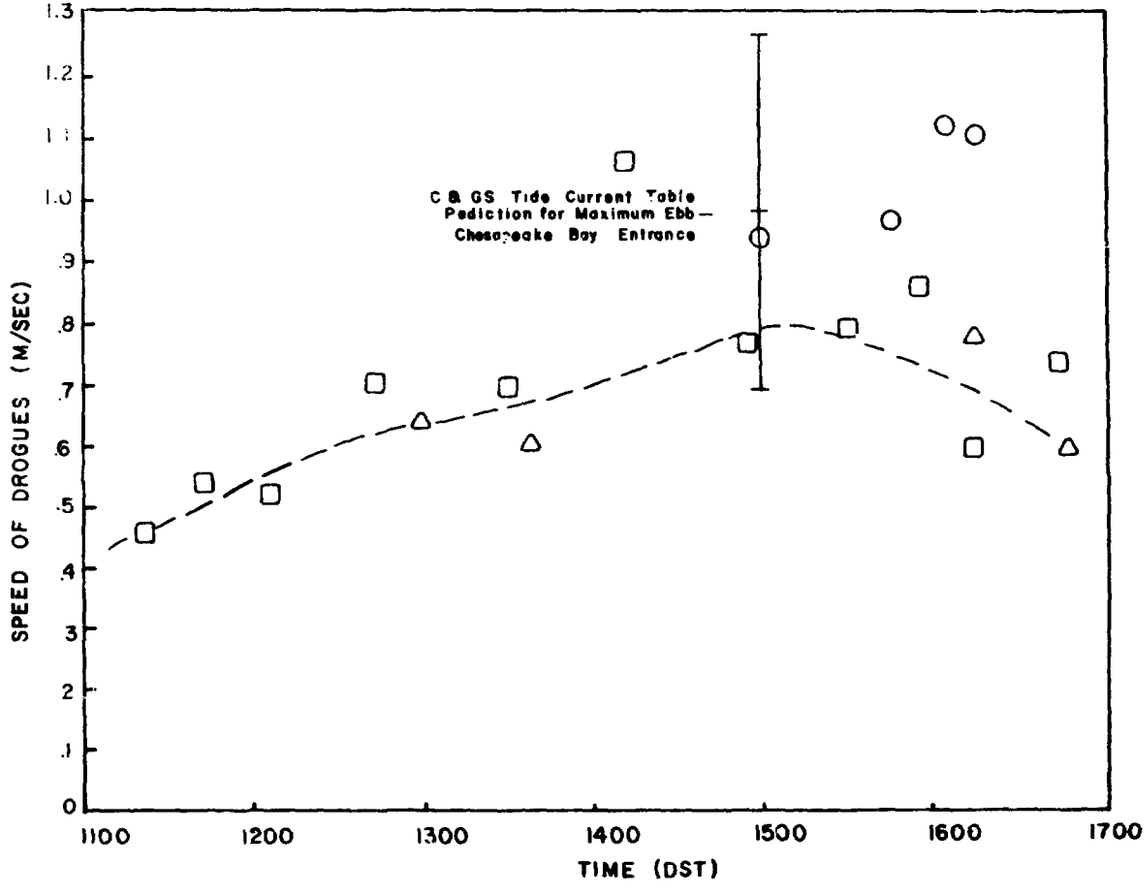


Figure 5.2. SKYLAB Support, Calculated Speeds.

## REFERENCES


Byrne, R. J., P. Bullock, and D. C. Tyler. 1973. Response characteristics of a tidal inlet: A case history. VIMS Contribution No. 580. Proc. of the 2nd Internat'l. Estuarine Res. Conf., Myrtle Beach, S. C. (in press).

Byrne, R. J., and M. Penney. 1974. Determination of tidal volumes in Barrier Island systems by sequential black and white IR imagery. In: Final Report for NASA/Wallops Contract NAS6-1902.

Cameron, H. L. 1952. The measurement of water current velocities by parallax methods. Journal of Photogrammetric Engineering, 18, pp. 99-104.

DeAlteris, J. T., and R. J. Byrne. 1973. The recent history of Wachapreague Inlet, Virginia. VIMS Contribution No. 573. Proc. of the 2nd Internat'l. Estuarine Res. Conf., Myrtle Beach, S. C. (in press).

Djuric', Dusan and Henri R. Leribaux. 1974. On the determination of turbulent diffusivity in shallow waters by aerial photography of floating markers. Limnology and Oceanography 19(1), pp. 138-144.

Groen, P., I. Claessen, A. J. Meerburg, and L. Otto. 1971. Measurements of deformation by turbulent motion in the sea and eddy diffusivities derived therefrom. Netherlands Journal of Sea Research 5(2), pp. 267-274.

Monahan, E. C., G. T. Kaye, and E. D. Michelena. 1973. Drogue measurements of the circulation in Grand Traverse Bay, Lake Michigan. University of Michigan Sea Grant Technical Report 35.

Strickland, J. D. H., and T. R. Parsons. 1968. A practical handbood of seawater analysis. Bull. Fisheries Res. Bd. Can., 167.

Welch, C. S., and L. Haas. 1973. Application of remote sensing to study nearshore circulation. First Annual Report for Grant NASA-NGL-47-022-005.

Yeske, L. A., T. Green, III, F. Scarpace, and R. E. Terrell. 1973. On current measurements in Lake Superior by Photogrammetry. Journal of Physical Oceanography 3(1), pp. 165-167.